

# Dual control of pcdh8l/PCNS expression and function in *Xenopus laevis* neural crest cells by adam13/33 via the transcription factors tfap2 $\alpha$ and arid3a

Vikram Khedgikar<sup>1</sup>, Genevieve Abbruzzese<sup>2</sup>, Ketan Mathavan<sup>1,3</sup>, Hannah Szydlo<sup>1</sup>, Helene Cousin<sup>1</sup>, Dominique Alfandari<sup>1,3\*</sup>

<sup>1</sup>Department of Veterinary and Animal Sciences, University of Massachusetts, Amherst, United States; <sup>2</sup>David H. Koch Institute for Integrative Cancer Research, Massachusetts Institute of Technology, Cambridge, United States; <sup>3</sup>Molecular and Cellular Biology graduate program, University of Massachusetts, Amherst, United States

**Abstract** Adam13/33 is a cell surface metalloprotease critical for cranial neural crest (CNC) cell migration. It can cleave multiple substrates including itself, fibronectin, ephrinB, cadherin-11, pcdh8 and pcdh8l (this work). Cleavage of cadherin-11 produces an extracellular fragment that promotes CNC migration. In addition, the adam13 cytoplasmic domain is cleaved by gamma secretase, translocates into the nucleus and regulates multiple genes. Here, we show that adam13 interacts with the arid3a/dril1/Bright transcription factor. This interaction promotes a proteolytic cleavage of arid3a and its translocation to the nucleus where it regulates another transcription factor: tfap2 $\alpha$ . Tfap2 $\alpha$  in turn activates multiple genes including the protocadherin pcdh8l (PCNS). The proteolytic activity of adam13 is critical for the release of arid3a from the plasma membrane while the cytoplasmic domain appears critical for the cleavage of arid3a. In addition to this transcriptional control of pcdh8l, adam13 cleaves pcdh8l generating an extracellular fragment that also regulates cell migration.

DOI: <https://doi.org/10.7554/eLife.26898.001>

\*For correspondence:  
alfandar@vasci.umass.edu

**Competing interests:** The authors declare that no competing interests exist.

**Funding:** See page 17

**Received:** 16 March 2017

**Accepted:** 21 August 2017

**Published:** 22 August 2017

**Reviewing editor:** Richard M White, Memorial Sloan Kettering Cancer Center, United States

© Copyright Khedgikar et al. This article is distributed under the terms of the [Creative Commons Attribution License](#), which permits unrestricted use and redistribution provided that the original author and source are credited.

## Introduction

Cranial neural crest (CNC) cells are a transient population of natural stem cells that are induced at the border of the neural and non-neural ectoderm by a combination of signals including BMP, Wnt and FGF (Dorsky et al., 1998; Monsoro-Burq et al., 2003; Tribulo et al., 2003). These signals mediate the expression of key transcription factors that define placodal and neural crest cells (Groves and LaBonne, 2014; Milet and Monsoro-Burq, 2012). Among those the transcription factor tfap2 $\alpha$  is one of the earliest and most conserved factors that controls the fate of neural border cells and later neural crest cells (de Croze et al., 2011). While loss of tfap2 $\alpha$  in all vertebrates tested leads to craniofacial defects, mutations in the tfap2 $\alpha$  gene in humans are associated with the Branchiooculofacial Syndrome highlighting the importance of this gene for craniofacial development and neural crest cell biology throughout evolution (Hoffman et al., 2007; Luo et al., 2003; Martinelli et al., 2011; Meshcheryakova et al., 2015; Van Otterloo et al., 2012).

Once induced, CNC cells migrate toward the ventral side of the embryo to contribute to most of the craniofacial structures. Many proteins have been shown to contribute to CNC migration, including multiple cell adhesion molecules such as integrins, cadherins and protocadherins, as well as cell surface metalloproteases that can effectively modulate these adhesion molecules (Alfandari et al.,

2010). In particular, while cadherin-11 is required at the surface of CNC, an excess of the protein prevents migration (Borchers et al., 2001). The cytoplasmic domain of cadherin-11 binds to the GEF trio and promotes filopodia formation in the migrating CNC (Kashef et al., 2009). In addition, cadherin-11 also localizes to nascent focal adhesion and interacts with the proteoglycan syndecan-4 via its transmembrane domain (Langhe et al., 2016). Lastly, the extracellular domain of cadherin-11 is cleaved by the metalloprotease adam13 producing an extracellular fragment that promotes cell migration (McCusker et al., 2009). This fragment can compete with the integral cadherin-11 to decrease contact inhibition of locomotion by a homophilic-dependent binding site, but this site is not required for its ability to promote CNC migration (Abbruzzese et al., 2016).

Other cadherin superfamily members are cleaved by ADAM metalloproteases. In *Xenopus*, the protocadherin pcdh8l is essential for CNC migration both in vivo and in vitro suggesting that it affects the basic cell locomotion machinery (Rangarajan et al., 2006). Interestingly, the protocadherin pcdh8 (PAPC), which can functionally replace pcdh8l in the neural crest cells (Schneider et al., 2014) is a substrate for adam13 (Abbruzzese et al., 2014). In chick, cleavage of cadherin-6 by adam10 and adam19 is also critical for proper migration of the neural crest cells (Schiffmacher et al., 2014). Thus, controlled expression of cadherin and protocadherin combined with proteolytic processing of these cell adhesion molecules appears to play a critical role in neural crest cell migration.

In addition to its proteolytic cleavage of cadherin-11, adam13/33 has been shown to play critical roles in CNC induction in *Xenopus tropicalis* by cleaving ephrinB, reducing its inhibitory activity upon the Wnt signaling pathway and allowing for a robust expression of *snai2* (Wei et al., 2010). In contrast, knock down of adam13 in *Xenopus laevis* has no effect on *snai2* expression but affects CNC migration in vivo (Cousin et al., 2011; Alfandari et al., 2001; Cousin et al., 2012). While the proteolytic role of adam13 is clearly important, the role of its cytoplasmic domain is also critical. We have shown that the cytoplasmic domain of adam13 is cleaved by gamma secretase and translocates into the nucleus where it regulates the expression of thousands of genes. The cleavage by gamma secretase requires a self-proteolytic cleavage by adam13 in its own cysteine rich domain and is therefore dependent on the adam13 proteolytic activity. In the absence of the cytoplasmic domain, adam13 cannot support CNC migration, but addition of a soluble form of its cytoplasmic domain fused to GFP, which partition exclusively in the nucleus, rescues cell migration. Similarly, addition of a single leucine in the cytoplasmic domain of adam13 that creates a nuclear export signal prevents adam13 ability to rescue CNC migration. This ability to regulate cell migration and gene expression is shared by the cytoplasmic domains of adam13 orthologues from *C.elegans* to marsupial, as well as the cytoplasmic domains of adam19 from frog and mouse, demonstrating the evolutionary conservation of this role. In contrast, the cytoplasmic domains of adam9 and adam10, which also translocate into the nucleus, cannot compensate for the loss of the adam13 cytoplasmic domain, revealing the specificity of this activity (Cousin et al., 2011).

Because, the cytoplasmic domain of adam13 does not possess any sequence similarity with transcription factors. We have investigated how it can modulate the expression of so many target genes. Here, we show that adam13 regulates the expression of the transcription factor *tfap2 $\alpha$* , which in turn regulates the protocadherin pcdh8l, a target of adam13 critical for CNC migration. We further show that adam13 physically interacts with the transcription factor *arid3a/dril1/BRIGHT*. This transcription factor is required for adam13's ability to induce *tfap2 $\alpha$* . In human Hek293T cells, adam13 stimulates the production of a shorter fragment of *arid3a* at the plasma membrane, which translocates to the nucleus. The production of the shorter fragment depends on the adam13 cytoplasmic domain, while the translocation from the membrane depends on the adam13 proteolytic activity. We propose that adam13 may interact with *arid3a* at the plasma membrane providing a pool of transcription factor that can be released upon cleavage of the adam13 cytoplasmic domain. This function is likely conserved and could contribute to many of the biological processes that are regulated by ADAM proteins (Alfandari et al., 2009; Dreymueller et al., 2012; Giebeler and Zigrino, 2016; Lu et al., 2008; Pollheimer et al., 2014; Reiss and Saftig, 2009).

## Results

### Adam13 cleaves pcdh8l

We have previously shown that adam13 cleaves the protocadherin pcdh8 (Abbruzzese *et al.*, 2014). Given the similarity in sequence between pcdh8 and pcdh8l and the critical role that pcdh8l plays during CNC migration, we hypothesized that adam13 may also cleave pcdh8l. To test this hypothesis, we co-transfected an N-terminal flag-tagged-pcdh8l (Figure 1A) along with either adam13 (A13) or a proteolytically inactive mutant form adam13E/A (A13E/A) in human Hek293T cells. Western blot analysis of conditioned media from transfected cells shows the presence of the extracellular fragment of pcdh8l only when co-transfected with adam13 (Figure 1B). The approximate size of the

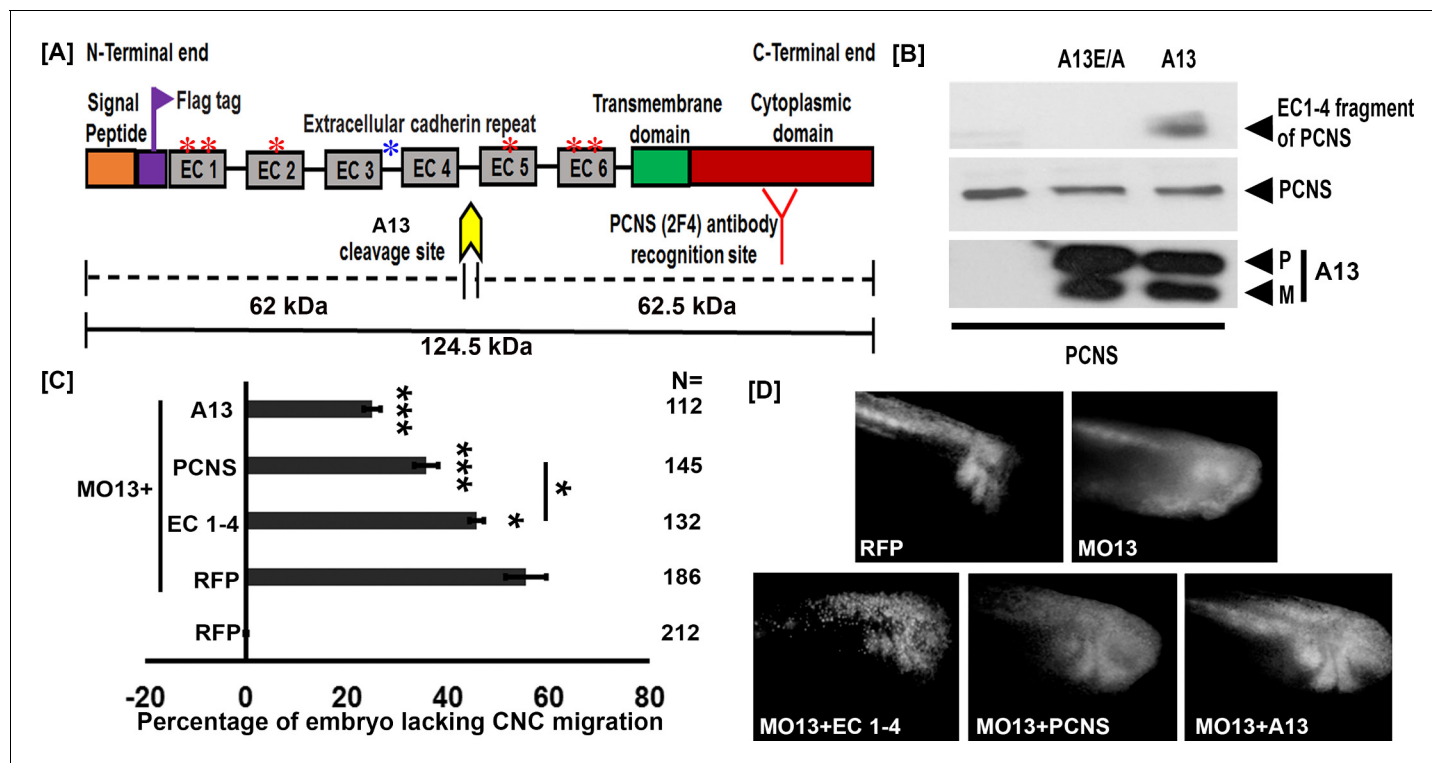


**Figure 1.** adam13 cleaves pcdh8l. (A) Schematic representation of full length pcdh8l. A Flag tag (DYKDDDDK) was introduced just before the first cadherin repeat (EC1). The yellow arrow indicates the predicted cleavage site of adam13 based on the molecular weight of N- and C- terminal fragments. Red and blue asterisk indicate N and O glycosylation site, respectively. The monoclonal antibody 2F4 was produced against the cytoplasmic domain (Red). (B) Western blot from transfected Hek293T cells. Glycoproteins from the conditioned media were purified on concanavalin-A agarose. The cleavage fragment was detected using the N-terminus Flag tag with the mAb M2. Total pcdh8l and adam13 were detected using mAb 2F4 and mAb 4A7, respectively. The Pro (P) and Metalloprotease (M) active forms of adam13 are indicated. (C) Histogram representing the percentage of embryos lacking fluorescent neural crest cell in the migration pathway. (D) Photographs of representative embryos with or without fluorescent migrating neural crest cells. Embryos were injected at the one-cell stage with a morpholino targeting adam13 (10 ng MO13). Messenger RNA for RFP alone or combined with the different constructs was injected at the 8-cell-stage in a dorsal animal blastomere. Each injection was compared to RFP injected in control embryos in which RFP positive cranial neural crest cells have successfully migrated into the branchial and hyoid arches (0% inhibition). N = number of embryos scored from three or more independent experiments. Error bars represent standard error to the mean. One-way ANOVA was performed to determine statistical significance. Statistically significant at \* $p < 0.05$ , \*\*\* $p < 0.005$ .

DOI: <https://doi.org/10.7554/eLife.26898.002>

The following source data and figure supplements are available for figure 1:

**Source data 1.** Source data for Figure 1.

DOI: <https://doi.org/10.7554/eLife.26898.005>

**Figure supplement 1.** Characterization of mAb 2F4 to pcdh8l.

DOI: <https://doi.org/10.7554/eLife.26898.003>

**Figure supplement 2.** adam13 overexpression increases pcdh8l fragments.

DOI: <https://doi.org/10.7554/eLife.26898.004>

fragment (>60 kDa) suggests that it includes the cadherin repeats 1 to 4 of pcdh8l (EC1-4). This was confirmed by generating a truncated form of pcdh8l including these domains, which migrates at the same position as the cleaved fragment (data not shown). No fragment was observed when pcdh8l was co-transfected with A13E/A suggesting that the proteolytic activity of adam13 is responsible for the cleavage of pcdh8l. To confirm these findings *in vivo*, we generated a monoclonal antibody to the cytoplasmic domain of pcdh8l (mAb 2F4). This antibody recognizes a protein of the appropriate size (120 kDa), expressed at the appropriate stage (stage 20), localized to the CNC in whole mount immunostaining and to the plasma membrane of CNC cells *in vitro*. We further confirmed that it recognizes pcdh8l but not pcdh8 transfected in Hek293T cells (**Figure 1—figure supplement 1**). At stage 20, the main protein recognized is the full length at 120 kDa, but two minor shorter fragments can be seen at  $\approx 60$  (1) and  $\approx 40$  kDa (2), respectively (**Figure 1—figure supplement 2**). These fragments increased in embryos injected with the adam13 mRNA suggesting that adam13 can also cleave pcdh8l *in vivo*.

### The pcdh8l fragment can partially compensate for the loss of adam13

Adam13 cleaves cadherin-11 to generate a fragment that promotes CNC migration (**McCusker et al., 2009; Abbruzzese et al., 2016; Cousin et al., 2011**). To test if the extracellular fragment of pcdh8l also regulates CNC migration we attempted to rescue the CNC migration defect induced by the loss of adam13 by expressing various forms of pcdh8l. To that effect, we injected an antisense morpholino oligonucleotide known to block adam13 translation (MO13) (**McCusker et al., 2009**) at the one-cell stage and the various mRNA at the 8-cell-stage in a dorsal animal blastomere (**Moody, 1987**). A lineage tracer (RFP mRNA) was co-injected in all cases to follow the migration of the CNC as previously described (**McCusker et al., 2009; Abbruzzese et al., 2016; Abbruzzese et al., 2014; Cousin et al., 2011; Cousin et al., 2012**). When MO13 is injected alone 57% of the embryos show no fluorescent CNC in the migration pathways (**Figure 1C–D**). Injection of a MO13-resistant adam13 mRNA significantly rescued CNC migration (26% inhibition). Injection of the pcdh8l extracellular fragment (EC1-4) mRNA rescued CNC migration significantly (47% inhibition), but less efficiently than the adam13 mRNA. Surprisingly, we found that loss of adam13 could be significantly rescued by the full length pcdh8l mRNA even more efficiently (36% inhibition) than with EC1-4, a phenomenon that was not observed for cadherin-11 (**McCusker et al., 2009**). These results suggest that the loss of adam13 does not simply prevent the cleavage of pcdh8l but could also affect its expression, localization or function.

### Adam13 regulates pcdh8l expression

We first tested if the loss of adam13 affects pcdh8l expression. For this, MO13 (10 ng) was injected at the one-cell-stage, embryos were raised until stage 20 when pcdh8l expression is maximal (**Rangarajan et al., 2006**), at which time mRNA and protein were extracted for analysis. In these conditions adam13 Knockdown (KD), which reduces the adam13 protein to undetectable levels (**Figure 2C,A13 Pro-P and Mature-M**) reduced the expression of pcdh8l mRNA by 43% (**Figure 2A**). To confirm this data, we injected MO13 (5 ng) into one blastomere of two-cell-stage embryos. The embryos were then fixed and stained by *in situ* hybridization with a pcdh8l probe. We observed that at stage 20, 71% of the embryos showed a reduced expression of pcdh8l on the injected side when compared to the non-injected control side (**Figure 2B**, N = 31). We also tested the protein level of pcdh8l by western blot, using mAb 2F4 (**Figure 2C**). When compared to non-injected embryos, the level of pcdh8l protein was significantly reduced. Because both adam13 and pcdh8l are also expressed in the somites, we tested if the reduction of pcdh8l was detectable in isolated CNC explants. CNC isolated from embryos injected with MO13 had a 36% reduction of pcdh8l mRNA compared to control CNC (**Figure 2—figure supplement 1A**). Again, western blot analysis with 2F4 showed a similar trend for the pcdh8l protein (**Figure 1—figure supplement 1B**). These results show that loss of adam13 results in a significant decrease of pcdh8l expression.

To test if adam13 could induce pcdh8l, we injected mRNA encoding either the wild-type adam13 or various mutant forms of the protein at the one-cell stage and dissected the naïve ectoderm (animal cap, AC) at stage 9. The animal cap explants were then grown until the control embryos reached neurula stage (17 to 20) and mRNA and protein expression were assessed by real-time PCR and western blot respectively. Analysis of mRNA levels show that wild-type adam13 induces pcdh8l

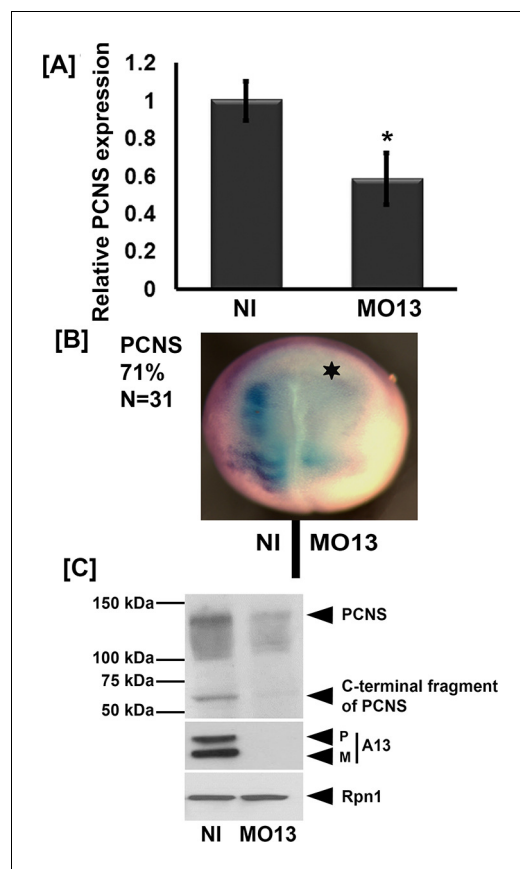


**Figure 2.** Adam13 knockdown reduces pcdh8l expression. (A) Relative mRNA expression of pcdh8l normalized to GAPDH obtained by real-time PCR. MO13 was injected at the one cell stage (10 ng) and embryos were collected at stage 20. Polyadenylated mRNA was extracted from non-injected and MO13 injected embryos (five embryos each). (B) Representative images of whole mount in situ hybridization in which MO13 (5 ng) was injected into one of the two blastomeres and non-injected side serves as control. Image shows reduced mRNA levels of pcdh8l in MO13 injected side (star, 71% of 31 embryos). (C) Western blot on glycoproteins isolated from either control (Non Injected) or knock down (10 ng MO13) stage 20 embryos (25 embryos each). MO13 efficiently prevents the translation of adam13 (A13) as well as reduces the pcdh8l protein level. A monoclonal antibody to *Xenopus* Ribophorin 1 (Rpn1) was used as a loading control. Error bars represent standard error to the mean (Mean  $\pm$  S.E.M). One-way ANOVA was performed to determine statistical significance. Statistically significant at \* $p < 0.05$ .

DOI: <https://doi.org/10.7554/eLife.26898.006>

The following source data and figure supplements are available for figure 2:

**Source data 1.** Source data for **Figure 2**.

DOI: <https://doi.org/10.7554/eLife.26898.009>

**Figure supplement 1.** adam13 knockdown reduces pcdh8l expression in cranial neural crest (CNC) cells.

Figure 2 continued on next page

expression whereas its catalytically inactive form (A13E/A), a mutant lacking the cytoplasmic domain ( $\Delta$ Cyto) and the isolated cytoplasmic domain (C13) all fail to induce expression of pcdh8l (**Figure 3A**). These results were confirmed at the level of pcdh8l protein expression using mAb 2F4 (**Figure 3B**). These results show that adam13 can induce the expression of pcdh8l in naïve ectoderm and that both the proteolytic activity and the cytoplasmic domain are required for this function.

## Adam13 regulates tfap2 $\alpha$ expression

We have previously shown that adam13 can regulate multiple genes including the cytoplasmic protease Capn8a (**Cousin et al., 2011**). While we showed that the cytoplasmic domain of adam13 is cleaved and translocates into the nucleus, there are no known DNA-binding motifs or transactivation domains in its sequence. For this reason we tested whether adam13 could regulate the expression of a transcription factor known to activate the expression of Cpn8a and pcdh8l. Tfap2 $\alpha$  is such a transcription factor, and it plays a key role in neural plate border specification where adam13 is expressed prior to neural crest migration (**de Croz e et al., 2011; Luo et al., 2005; Alfandari et al., 1997**). As described above for pcdh8l, we used the morpholino to adam13 to inhibit adam13 translation in embryos and collected them at stage 20. The real-time PCR data indicate that MO13 reduces tfap2 $\alpha$  mRNA expression to 67% of control embryos (**Figure 4A**). In situ hybridization with a tfap2 $\alpha$  probe shows that loss of adam13 reduces tfap2 $\alpha$  mRNA expression on the injected side in 76% of the embryos (**Figure 4B**). To test if adam13 could regulate the tfap2 $\alpha$  promoter, we cloned 2.5 Kbp of the *Xenopus laevis* genomic sequence upstream of the transcription start of the tfap2 $\alpha$  gene into a luciferase vector (pGlo3, Bio-rad). We then injected at the 8-cell-stage in the dorsal animal blastomere the tfap2 $\alpha$ :luciferase plasmid together with a Renilla control plasmid in both control embryos and embryos lacking adam13. Analysis of the luciferase activity in dissected CNC explants shows a significant reduction of the tfap2 $\alpha$  promoter activity following adam13 KD (**Figure 4C**). This decrease is nearly identical to the observed reduction of the endogenous tfap2 $\alpha$  mRNA (**Figure 4A**) suggesting that this reporter contains the key responsive elements regulated by adam13.

Figure 2 continued

DOI: <https://doi.org/10.7554/eLife.26898.007>**Figure supplement 1—source data 1.**Source data for **Figure 2—figure supplement 1.**DOI: <https://doi.org/10.7554/eLife.26898.008>

and cultured until sibling embryos reached neurula stage (17 to 20) to isolate mRNA for real-time PCR. The results show that compared to non-injected control (NI), animal caps injected with adam13 RNA have a significant increase in tfap2 $\alpha$  mRNA expression levels (**Figure 5A**). Similar to what was observed for pcdh8l, both the cytoplasmic domain and the proteolytic activity of adam13 are required for the full expression of tfap2 $\alpha$ .

We then used the tfap2 $\alpha$ :luciferase construct to test if adam13 could induce tfap2 $\alpha$  expression in Human Hek293T cells. As seen in **Figure 5B**, transfection of adam13 results in an almost 4-fold increase in tfap2 $\alpha$  promoter activity. We previously showed that the cytoplasmic domains of adam13 and 19 could rescue CNC migration in embryos expressing adam13 lacking a cytoplasmic domain ( $\Delta$ Cyto), while the cytoplasmic domain of adam9 could not. In addition both adam13 and 19 cytoplasmic domains could rescue the expression of Cpn8a in CNC while adam9 could not (**Cousin et al., 2011**). We therefore tested the ability of adam9, 13 and 19 to induce the tfap2 $\alpha$  promoter (**Figure 5B**). As expected, only adam13 and adam19 could induce the expression of tfap2 $\alpha$  while adam9 could not. In addition, the cytoplasmic domain of adam13 was critical for tfap2 $\alpha$  induction. As seen for pcdh8l, the cytoplasmic domain alone was not able to induce tfap2 $\alpha$  expression. In contrast to what was seen in the animal cap, the proteolytically inactive adam13 (A13E/A) mutant was able to induce the reporter even if less efficiently than the wild type adam13.

### Adam13 regulation of pcdh8l depends on tfap2 $\alpha$

To test if tfap2 $\alpha$  was involved in adam13 induction of pcdh8l, we expressed adam13 in animal cap with or without knocking down tfap2 $\alpha$ . As seen before, injection of adam13 results in an increase in expression of pcdh8l and tfap2 $\alpha$  mRNA (**Figure 5C and D**). In contrast, injection of a tfap2 $\alpha$  morpholino prevented the induction of both pcdh8l and tfap2 $\alpha$  by adam13 (**Figure 5C and D**). In *Xenopus tropicalis*, adam13 has been shown to positively regulate the Wnt signaling pathway (**Wei et al., 2010**) and Wnt/ $\beta$ -catenin has been shown to regulate tfap2 $\alpha$ . To test if adam13 control of pcdh8l or

### The adam13 cytoplasmic domain is critical for tfap2 $\alpha$ induction

Given that adam13 is required for proper tfap2 $\alpha$  expression, we then tested if adam13 expression in naïve ectoderm could induce tfap2 $\alpha$  expression. Again, we injected embryos at the one cell-stage with the various constructs. Animal caps were dissected at the blastula stage

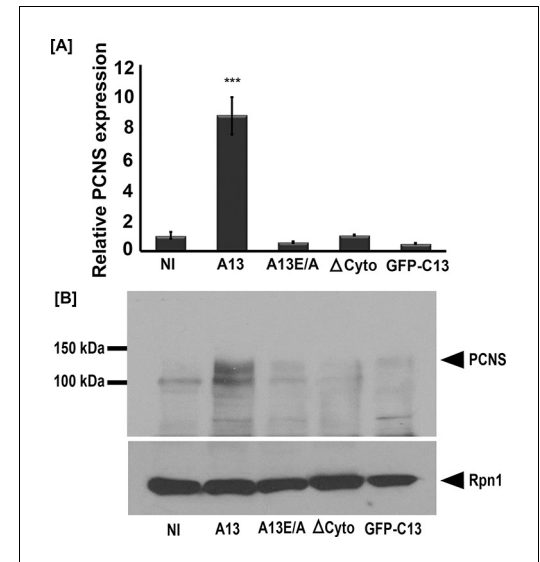


**Figure 3.** Full-length adam13 induces pcdh8l expression in naïve ectoderm (animal cap cells). One-cell stage embryos were injected with mRNA encoding various forms of adam13 (1 ng). Animal cap (AC) explants were dissected at stage 9 and grown in 0.5X MBS until sibling embryos reached stage 18 to 20. mRNA and protein was extracted from AC for analysis of pcdh8l. (A) Quantitative real-time PCR from mRNA isolated from 10 animal caps. The relative level of pcdh8l expression was normalized to GAPDH. (B) Western blot for pcdh8l protein using mAb2F4. 30 AC were used to extract protein from embryos injected with various adam13 constructs. Western blot shows induction of pcdh8l by full-length adam13, whereas other constructs fails to induce pcdh8l expression. adam13 (A13), non proteolytic adam13 (A13E/A), adam13 lacking a cytoplasmic domain ( $\Delta$ Cyto), isolated adam13 cytoplasmic domain (GFP-C13). Error bars represent standard error to the mean (Mean  $\pm$  S.E.M). One-way ANOVA was performed to determine statistical significance. Statistically significant at \*\*\* $p$ <0.001.

DOI: <https://doi.org/10.7554/eLife.26898.010>

The following source data is available for figure 3:

**Source data 1.** Source data for **Figure 3.**DOI: <https://doi.org/10.7554/eLife.26898.011>

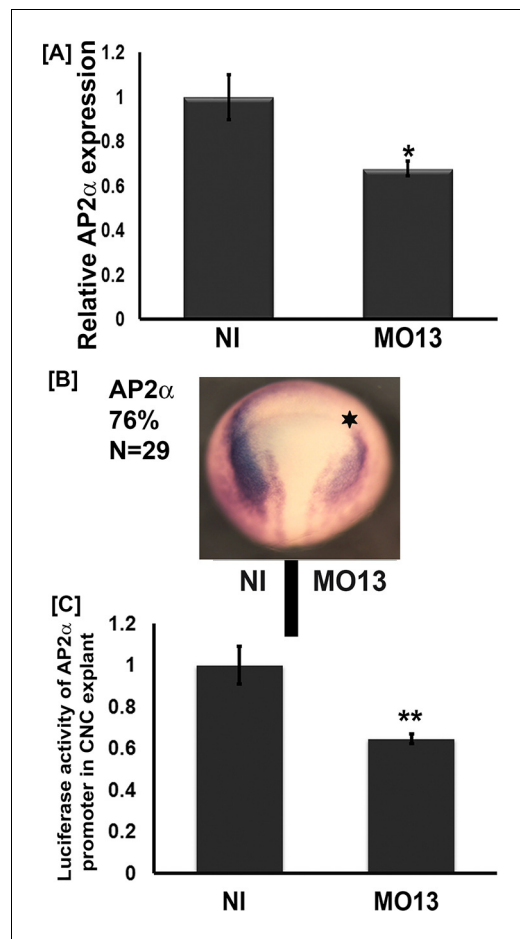


**Figure 4.** Adam13 knockdown reduces *tfap2α* expression. (A) Relative mRNA expression of *AP2α* normalized to *GAPDH* (five embryos). Real-time PCR analysis shows a 40% decrease in *AP2α* expression in response to *adam13* KD (B) Representative images of dorsal view of whole mount in situ hybridization with *AP2α*. MO13 (5 ng) was injected in one of the two blastomeres (star). The non-injected side serves as control. *adam13* KD reduces *AP2α* expression in 76% of the embryos (N = 29). (C) Luciferase activity of *AP2α* promoter in cranial neural crest cells (CNC). One-cell stage embryos were injected with MO13 (10 ng). Control and KD embryos were further injected at the 8 cell stage with the *AP2α*:luciferase reporter (100 pg) together with pRL-CMV (10 pg) in one animal dorsal blastomere. CNC explants were dissected from stage 15–17 embryos and individual explants were lysed to measure luciferase activity. The normalized values from 10 individual explants (two biological replicates) were used for each measure. Error bars represent standard error to the mean (Mean  $\pm$  S.E.M). One-way ANOVA was performed to determine statistical significance. Statistically significant at \* $p < 0.05$ , \*\* $p < 0.01$ . DOI: <https://doi.org/10.7554/eLife.26898.012>

The following source data is available for figure 4:

**Source data 1.** Source data for **Figure 4**.

DOI: <https://doi.org/10.7554/eLife.26898.013>

*tfap2α* also involves this pathway, we injected embryos with a morpholino to  $\beta$ -catenin (Heasman *et al.*, 2000). The results show that reduction of  $\beta$ -catenin does not prevent *adam13* induction of *pcdh8l* or *tfap2α* (Figure 5C and D). Interestingly *adam13* up-regulation of *tfap2α* was also inhibited by the morpholino to *tfap2α* suggesting a positive feedback loop mechanism in which, *tfap2α* is involved in its own regulation by *adam13* (Figure 5D).

### Adam13 physically interacts with *arid3a* and *FoxD3*

Our results suggest that *adam13* can directly regulate the *tfap2α* promoter. However, there is no evidence that the cytoplasmic domain of *adam13* can interact with DNA. In addition, fusing the *adam13* cytoplasmic domain with the VP-16 trans-activator domain does not induce the expression of *tfap2α* (Alfandari, unpublished result). Taken together, these results suggest that *adam13* may interact with and regulate a transcription factor that controls *tfap2α* expression. To test this hypothesis, we narrow down the list of potential candidate transcription factors based on the presence of their binding site on the *tfap2α* promoter (Jaspar [Sandelin *et al.*, 2004]), their expression in the CNC (Xenbase, [Bowes *et al.*, 2010; Karpinka *et al.*, 2015]), and their ability to induce the *tfap2α* luciferase reporter in Hek293T cells (data not shown). We then tested whether any of these transcription factors could physically interact with *adam13*. Two transcription factors (*foxd3* and *arid3a*) were positive in all assays and were tested for *adam13* binding by co-immunoprecipitation (Figure 6). When injected into embryos, *arid3a*-flag co precipitated with *adam13* (Figure 6A). This interaction was lost when *adam13* was KD (MO13). Similarly when *foxd3*-myc RNA was injected in embryos either alone or with the *adam13* MO, the *foxd3* protein was co-precipitated with the endogenous *adam13* protein and was absent when *adam13* was KD (Figure 6B). These results show that both transcription factors can interact with *adam13* in vivo.

### *Arid3a* is critical for *tfap2α* and *pcdh8l* expression

We then tested whether *foxd3* and *arid3a* were required for *adam13* induction of *tfap2α* and *pcdh8l* using the animal cap assay (Figure 7A–B). The real-time PCR shows that while *arid3a* KD efficiently prevented *adam13* induction of both *tfap2α* and *pcdh8l*, *foxd3* KD had no effect. In

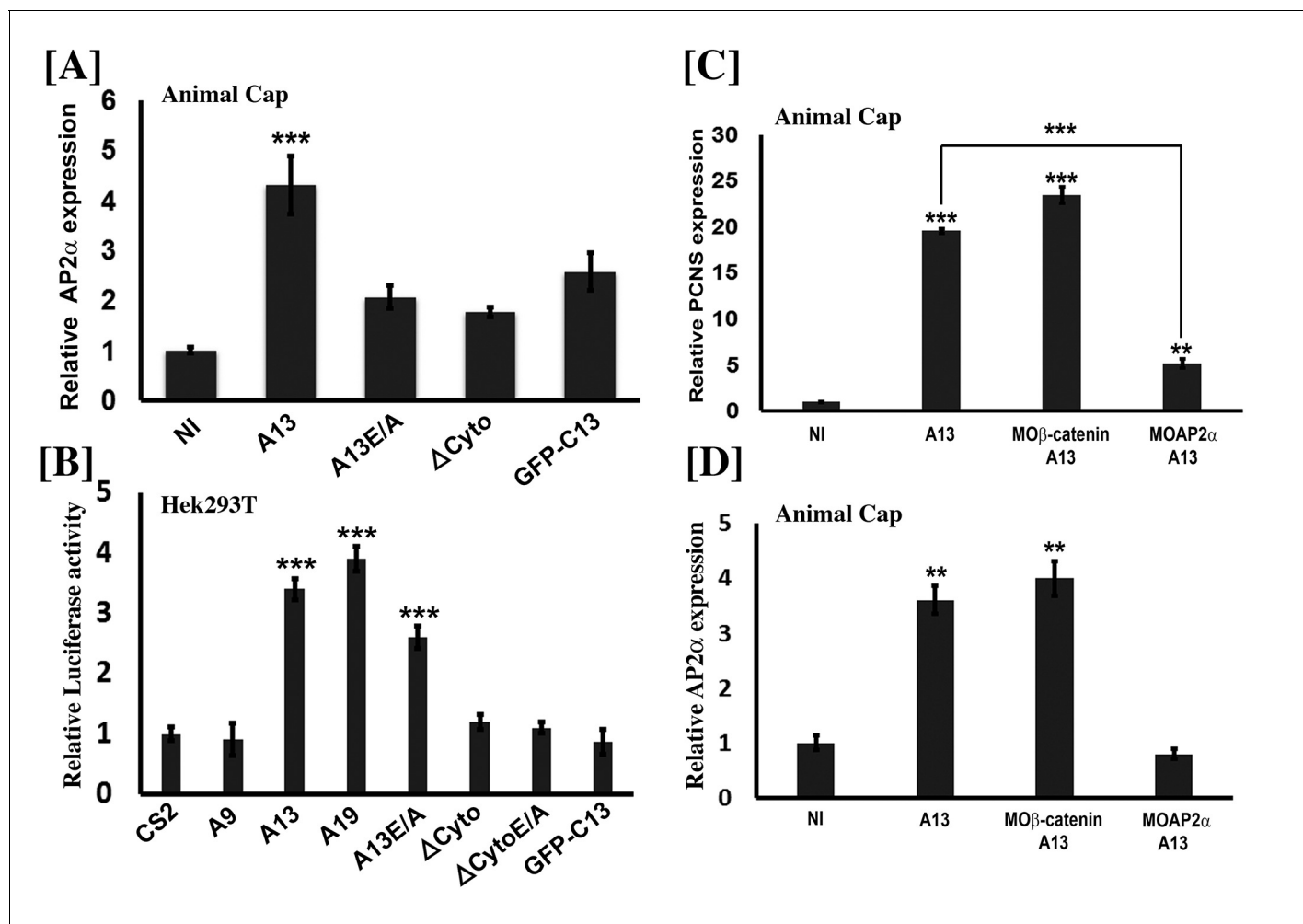


**Figure 5.** Adam13 induces pcdh8l via AP2 $\alpha$ . (A, C, D) Relative expression of AP2 $\alpha$  and pcdh8l in naïve ectoderm (animal cap) by real-time PCR. One-cell stage embryos were injected with 1 ng of the various adam13 constructs and morpholinos and embryos were collected at stage 9 to dissect animal cap cells (AC). AC were grown in 0.5X MBS until sibling embryos reached stage 20 to 22. Messenger RNA was extracted from 10 AC for gene expression analysis. Expression was normalized using GAPDH and compared to the expression in non-injected AC (NI). (A) Real-time PCR data show that adam13 can induce AP2 $\alpha$  by more than four fold. Both proteolytic activity and the presence of the cytoplasmic domain are essential for full activation. (B) Luciferase activity of AP2 $\alpha$  promoter in Hek293T cells shows induction by adam13 and ADAM19 but not ADAM9. For each transfection the luciferase values were normalized to the Renilla values driven by the CMV promoter. In these assays, the absence of proteolytic activity (A13E/A) reduced AP2 $\alpha$  induction only slightly, while the deletion of the cytoplasmic domain ( $\Delta$ Cyto) prevented the activity. (C) Induction of AP2 $\alpha$  by adam13 was prevented by the KD of AP2 $\alpha$  (10 ng of MOAP2 $\alpha$ ) but not  $\beta$ -catenin (20 ng of Mo $\beta$ -catenin). (D) Expression of AP2 $\alpha$  in response of adam13 also depends on AP2 $\alpha$  but not  $\beta$ -catenin. Error bars represent standard error to the mean (Mean  $\pm$  S.E.M). One-way ANOVA was performed to determine statistical significance. Statistically significant at \*\* $p < 0.01$ , \*\*\* $p < 0.001$ .

DOI: <https://doi.org/10.7554/eLife.26898.014>

The following source data is available for figure 5:

**Source data 1.** Source data for **Figure 5**.

DOI: <https://doi.org/10.7554/eLife.26898.015>

these experiments, loss or gain of adam13 function had no effect on arid3a and foxd3 expression (**Figure 7—figure supplement 1**).

Because arid3a was shown to regulate TGF $\beta$  signaling downstream of Smad2 (**Callery et al., 2005**) and the ability of mammalian ADAM12 to mediate TGF $\beta$  signaling (**Ruff et al., 2015**), we investigated whether adam13 induction of pcdh8l and tfap2 $\alpha$  requires Smad2. Animal cap experiments show that adam13 induces tfap2 $\alpha$  and pcdh8l expression even when Smad2 is knocked down (**Figure 8A–B**). In addition Smad2 does not induce the tfap2 $\alpha$  promoter in Hek293T cells and the

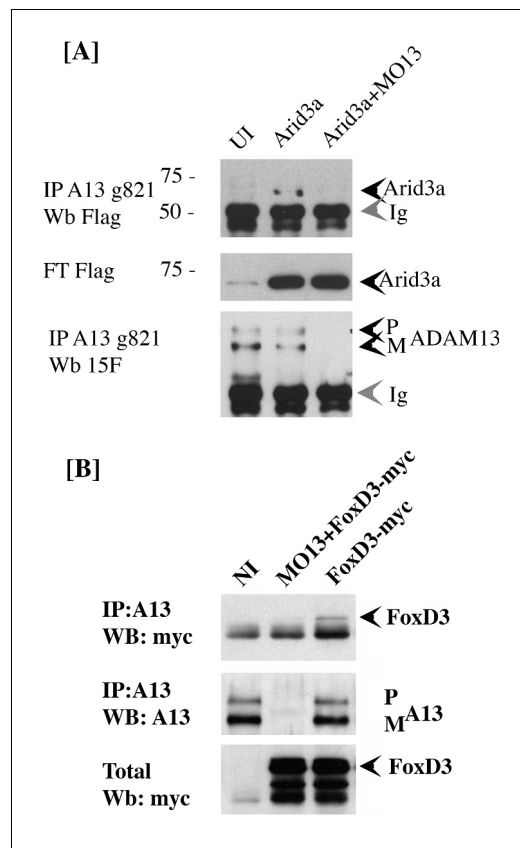


**Figure 6.** adam13 binds to arid3a and foxd3. (A) Co-immunoprecipitation of arid3a-flag with adam13. Arid3a-flag mRNA were injected in one-cell stage embryos either alone or with the morpholino to adam13 (MO13.) Proteins were immunoprecipitated with a goat polyclonal antibody directed against the cytoplasmic domain of adam13 (g821, [Cousin et al., 2011]) and blotted with M2 to detect the Flag-tag of arid3a. The flow through was used to detect arid3a. The immunoprecipitation were re-probed using 6615F to detect adam13 (Alfandari et al., 1997). (B) Co-immunoprecipitation of adam13 and FoxD3 from embryos. FoxD3-myc mRNA was injected at the one-cell stage either alone or with MO13. Adam13 was immunoprecipitated using the goat polyclonal antibody to adam13 (g821), and the proteins were detected by western blot using either the myc antibody (9E10) or a rabbit antibody to adam13 (6615F). FoxD3 co-precipitated with endogenous adam13. DOI: <https://doi.org/10.7554/eLife.26898.016>

expression pattern shows that it is expressed in the non-neural ectoderm and the neural plate border (Callery et al., 2005) where it overlaps with adam13 suggesting that it could play a role in neural crest specification. We, therefore, investigated the effect of the loss of arid3a on the expression of tfap2 $\alpha$ , pcdh8l and the neural crest marker snai2. To avoid a general defect in mesoderm patterning, we injected embryos at the 8-cell stage in a single dorsal animal blastomere and tested the expression of the selected genes by in situ hybridization (Figure 9A–C). The results show that loss of arid3a

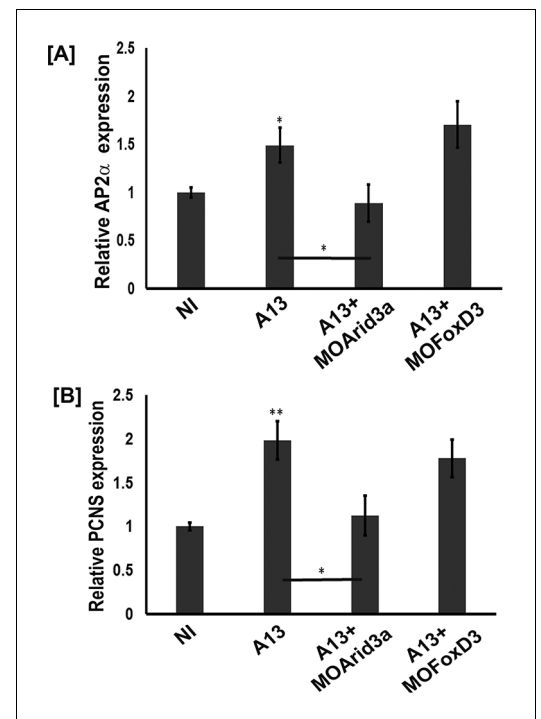


**Figure 7.** adam13 requires arid3a for induction of AP2 $\alpha$ . Relative expression of AP2 $\alpha$  (A) and pcdh8l (B) in animal caps from embryos injected with adam13 alone or with a morpholino to arid3a (20 ng) or FoxD3 (20 ng). Animal caps were extracted at stage 17. DOI: <https://doi.org/10.7554/eLife.26898.017>  
The following source data and figure supplements are available for figure 7:

**Source data 1.** Source data for Figure 7.

DOI: <https://doi.org/10.7554/eLife.26898.020>

**Figure supplement 1.** adam13 does not induce arid3a and FoxD3 expression in Naïve ectoderm.

DOI: <https://doi.org/10.7554/eLife.26898.018>

**Figure supplement 1—source data 1.** Source data for Figure 7—figure supplement 1.

DOI: <https://doi.org/10.7554/eLife.26898.019>

inhibitory Smad, Smad7 does not prevent adam13 induction of the tfap2 $\alpha$  promoter in the same cells (Figure 8C). These results suggest that adam13 regulation of tfap2 $\alpha$  does not involve the TGF $\beta$  signaling pathway.

While arid3a has been shown to be essential for mesoderm specification (Callery et al., 2005), there is no evidence concerning its role in neural crest cell induction or patterning. Published

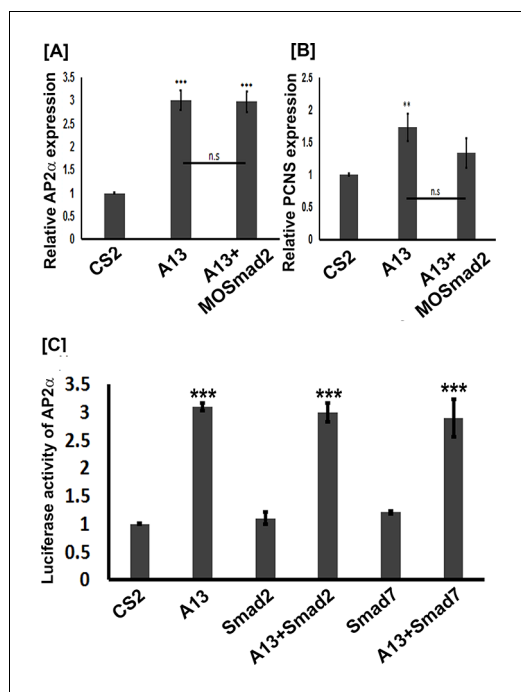


**Figure 8.** adam13 induction of AP2 $\alpha$  and pcdh8l does not involve Smad2. (A–B) Relative expression of AP2 $\alpha$  and pcdh8l in animal caps dissected from control embryos, or embryos injected with adam13 or adam13 and a morpholino to Smad2 (MOSmad2, 25 ng). (C) Luciferase assays in Hek293T cells show no induction of AP2 $\alpha$  promoter activity by Smad2 (0.5  $\mu$ g) or Smad 7 (0.5  $\mu$ g). Smad2 does not increase adam13 activation of the AP2 $\alpha$  promoter, while Smad7 does not reduce adam13 induction of AP2 $\alpha$  promoter. Smad2 and Smad7 were transfected with or without adam13 (0.5  $\mu$ g) along with AP2 $\alpha$  promoter-luciferase and the pRL-CMV (100 ng, 10  $\mu$ g). The ratio of luciferase to renilla was used to normalize each transfection to the empty vector control (CS2). Error bars represent standard error to the mean (Mean  $\pm$  S.E.M). One-way ANOVA was performed to determine statistical significance. Statistically significant at \*\* $p < 0.01$ , \*\*\* $p < 0.001$ .

DOI: <https://doi.org/10.7554/eLife.26898.021>

The following source data is available for figure 8:

**Source data 1.** Source data for **Figure 8**.

DOI: <https://doi.org/10.7554/eLife.26898.022>

as previously described for B-cells, and if adam13 and the various mutants affected this localization (**Figure 10C**). Transfected Arid3a was found in the membrane fraction of Hek293T cells in all conditions tested. In cells expressing adam13, the 40 kDa fragment of arid3a (arid3a Short) was enriched. This fragment was dramatically increased in cells expressing the A13E/A mutant, suggesting that the proteolytic activity of adam13 is not responsible for the production of arid3a Short. In contrast, cells expressing A13 $\Delta$ Cyto express the same level of arid3a Short than those expressing only arid3a. Taken together, these results show that adam13 regulates arid3a post-translational modification (proteolytic cleavage) and nuclear translocation. These results are compatible with a model (**Figure 11-1**) in which the adam13 cytoplasmic domain is part of a complex that either cleaves arid3a at

decreased the expression of tfap2 $\alpha$  and pcdh8l as expected but also snai2, suggesting a key role in neural crest cell patterning.

### Tfap2 $\alpha$ but not arid3a can rescue CNC migration in embryos lacking adam13

It is clear that adam13 regulates tfap2 $\alpha$  expression, and therefore, it is expected that restoring the level of tfap2 $\alpha$  in embryos lacking adam13 should at least partially rescue CNC migration. Indeed, injection of tfap2 $\alpha$  in embryos lacking adam13 significantly rescued CNC migration (**Figure 9E–F**) in a way similar to that of pcdh8l expression. In contrast, expression of arid3a had no effect on CNC migration in embryos lacking adam13. These results are consistent with a model where adam13 requires arid3a to function in the CNC. The facts that arid3a expression is not regulated by adam13 (**Figure 7—figure supplement 1**), that both proteins interact (**Figure 6**) and that arid3a cannot compensate for the loss of adam13 (**Figure 9E**) suggest that arid3a is not downstream of adam13 but rather that the two proteins work together.

### Adam13 stimulates Arid3a nuclear translocation

To test if adam13 could regulate Arid3a translocation to the nucleus, we performed nuclear and cytoplasmic fractionation of transfected Hek293T cells (**Figure 10**). As expected we found that arid3a is equally distributed between the cytoplasmic and nuclear compartment (**Figure 10A**). Interestingly, in the nucleus a smaller fragment (40 kDa) is observed, and this fragment is much more abundant in the nucleus of cells co-transfected with adam13. We then tested if this fragment was also observed in cells co-transfected with the adam13 protease dead mutant (A13E/A) and the mutant lacking the cytoplasmic domain (A13 $\Delta$ Cyto). In both conditions, we found that the fragment was not increased by these mutants (**Figure 10B**). We then tested if Arid3a was localized to the plasma membrane in Hek293T cells,

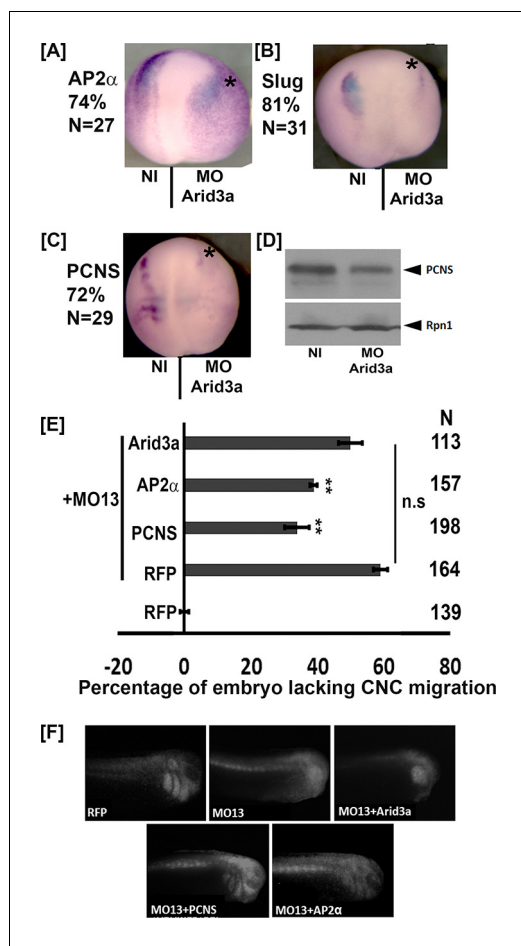


**Figure 9.** *arid3a* is critical for multiple gene expression in the CNC. (A–C) Representative dorsal view of neurula treated by whole mount in situ hybridization with probes for *tfap2 $\alpha$*  (AP2 $\alpha$ ), *snai2* (Slug) and *pcdh8l* (PCNS). Eight-cell stage embryos were injected in one dorsal animal blastomere with the *arid3a* morpholino (5 ng, Asterisk). The percentage of embryos with reduced signal in the injected side is given in N is the total number of embryos obtained from each case. (D) Western blot using mAb2F4 to detect *pcdh8l* (PCNS). Glycoproteins from 25 embryos were extracted and purify on ConA-agarose beads. Rpn1 was used as a loading control. (E) Histogram representing the percentage of embryos lacking CNC migration. One-cell stage embryos were injected with MO13. Control or KD embryos were further injected at the 8 cell stage in one animal dorsal blastomere with mRNA for RFP, PCNS, AP2 $\alpha$  or Arid3a. Observation of the RFP fluorescence at stage 24–26 reveals that the inhibition of migration by *adam13* KD is partially rescued by *pcdh8l* and AP2 $\alpha$  but not Arid3a. Error bars represent standard error to the mean (Mean  $\pm$  S.E.M). One-way ANOVA was performed to determine statistical significance. Statistically significant at \* $p < 0.05$ , \*\* $p < 0.01$ . (F) Representative examples of injected embryos. Posterior to the left, dorsal is up.

DOI: <https://doi.org/10.7554/eLife.26898.023>

Figure 9 continued on next page

the plasma membrane or stabilizes a cleaved form of *arid3a* (Figure 11-2). Upon *adam13* self-proteolysis (Cousin et al., 2011; Gaultier et al., 2002) (Figure 11), gamma secretase can cleave the cytoplasmic domain of *adam13* (Figure 11-3), which then translocates with or without *arid3a* to the nucleus (Figure 11-4). In the absence of *adam13* proteolytic activity, the complex remains stable at the plasma membrane (Figure 10C), while in the absence of the cytoplasmic domain the complex is not formed.

## Discussion

Our results show that *adam13* expression is essential for the proper expression of *tfap2 $\alpha$* , a transcription factor that defines the neural plate border in all vertebrates studied so far (de Croz  et al., 2011; Hoffman et al., 2007; Luo et al., 2003; Martinelli et al., 2011; Van Otterloo et al., 2012; Van Otterloo et al., 2010). This regulation is mediated by the interaction of *adam13* with the *arid3a* transcription factor and requires both the cytoplasmic domain and metalloprotease activity of *adam13* in na ve ectoderm. Our results suggest that the cytoplasmic domain of *adam13* is critical for either stabilizing or inducing the cleavage of *arid3a* at the plasma membrane. This fragment is then accumulated in the nucleus of cells co-transfected with *adam13*. The accumulation of this fragment in the nucleus appears to be controlled by the *adam13* proteolytic activity, as it is impaired in the A13E/A mutant. Given *adam13*'s ability to cleave itself within its cysteine rich domain (Gaultier et al., 2002), thus becoming a substrate for gamma-secretase, to cleave and release the cytoplasmic domain from the membrane (Cousin et al., 2011), we propose that the complex containing the cleaved *arid3a*, and at least the *adam13* cytoplasmic domain is then free to translocate into the nucleus (Figure 11). This model is consistent with the essential roles of both the proteolytic and cytoplasmic domain of *adam13* in animal cap and the CNC. It is also consistent with the observation that the GFP-C13 fusion protein containing the *adam13* cytoplasmic domain, which is found only in the nucleus, is unable to induce *tfap2 $\alpha$*  expression. On the other hand, the fact that the *adam13* E/A mutant can induce the reporter in Hek293T cells even at a lower efficiency is puzzling. While this construct clearly increases the *arid3a* fragment, it does not allow its efficient nuclear translocation (Figure 10B and C). One possible explanation is that it may act as a dominant mutant by trapping e2f1 at the plasma

Figure 9 continued

The following source data is available for figure 9:

**Source data 1.** Source data for **Figure 9**.

DOI: <https://doi.org/10.7554/eLife.26898.024>

cells, A13E/A could sequester E2F1 at the plasma membrane and increase the reporter activity. In *Xenopus*, e2f1 is expressed maternally and is strongly down regulated at stage 20 (Owens et al., 2016) when the animal caps are extracted. Thus, A13E/A expression would have no effect on its ability to translocate in the nucleus.

In B-cells, ARID3a also known as Bright, is post translationally modified. First, it is palmitoylated and associate with lipid raft at the plasma membrane (Schmidt et al., 2009). Upon stimulation of the B-cell receptor, arid3a is sumoylated, dissociate from the lipid raft and is then free to regulate gene expression (Prieur et al., 2009). It is possible that in the neural crest cells, adam13 regulates a pool of arid3a associated with lipid raft at the plasma membrane. It could do this by helping assemble the proper signaling complex including the enzyme responsible for arid3a post-translational modification. In the complex, the presence of a protease would cleave off the N-terminal domain of arid3a. This cleavage could be important for releasing a transcriptional inhibitor (e.g. e2f1) or simply destabilizing arid3a interaction with the plasma membrane. Given the widespread expression of arid3a, this would provide a mechanism by which the transcription factor is only activated in the right cells and at the right time. Our results show that adam13 expression dramatically increases the nuclear localization of a cleavage product of arid3a (arid3a Short), while it does not affect the overall distribution of the intact arid3a protein. This depends on both the proteolytic activity and the cytoplasmic domain of adam13. It is tempting to speculate that this fragment (arid3a Short), which has not been described before, is responsible for the increased expression of tfap2 $\alpha$ . Based on the calculated molecular weight of the fragment, it is likely to maintain the intact ARID (DNA binding) domain as well as the RECKLES domain that control the nuclear localization. It will be interesting to determine if adam13 stabilizes arid3a Short or produces it. If this model were correct, we would expect that proteins that interfere with the production of the cleaved cytoplasmic domain would also interfere with adam13's ability to induce tfap2 $\alpha$ . We have previously shown that the secreted Wnt receptor Fz4-v1, binds to adam13 and prevents its proteolytic activity. We further showed that KD of Fz4-v1 induces an early production of the adam13 cytoplasmic fragment (Abbruzzese et al., 2015). In embryos, KD of Fz4-v1, increases both tfap2 $\alpha$  and pcdh8l transcription (data not shown), while In Hek293T cells, expression of Fzd4-v1 inhibits adam13 activation of the tfap2 $\alpha$  reporter further supporting our model.

Our results also show that adam13 activation of tfap2 $\alpha$  in naïve ectoderm does not require  $\beta$ -catenin, while tfap2 $\alpha$  has been shown to be induced by  $\beta$ -catenin in the CNC (de Croz   et al., 2011). In addition, we also show that adam13 induction of tfap2 $\alpha$  requires the presence of tfap2 $\alpha$ . Both adam13 and tfap2 $\alpha$  are initially expressed in the entire ectoderm and become excluded from the neural plate to be restricted to the neural folds and later neural crest (Alfandari et al., 1997; Luo et al., 2002). In addition, the quantitative expression pattern of tfap2 $\alpha$  and adam13 by RNA-seq is nearly identical (Owens et al., 2016). This suggests that adam13 and tfap2 $\alpha$  expression is initially controlled by the same transcription factor possibly  $\beta$ -catenin (Deardorff et al., 2001), and that adam13 is later required for the maintenance and amplification of tfap2 $\alpha$  expression within the neural fold and neural crest cells. This is compatible with the fact that adam13 is not required for  $\beta$ -catenin induction of snai2 in the CNC in *Xenopus laevis*. Also consistent with this model, we find that both arid3a and tfap2 $\alpha$  can induce the tfap2 $\alpha$  reporter individually, and the combination of these two proteins produces an additive increase in the luciferase expression (data not shown). We also tested if adam13 could initiate a full CNC program in naïve ectoderm. We found that while snai2 and twist can be induced by adam13, cadherin 11, sox8 and sox10 were not (data not shown) suggesting that adam13 is not capable to induce neural crest cells from naïve ectoderm.

Ultimately, adam13 induction of tfap2 $\alpha$  results in the induction of pcdh8l and the up-regulation of Cpn8a in the CNC, two proteins critical for CNC migration. The fact that CNC lacking adam13 can migrate in vitro while those missing pcdh8l cannot (Rangarajan et al., 2006) might be explained by the observation that the CNC lacking adam13 eventually expresses both tfap2 $\alpha$  and pcdh8l

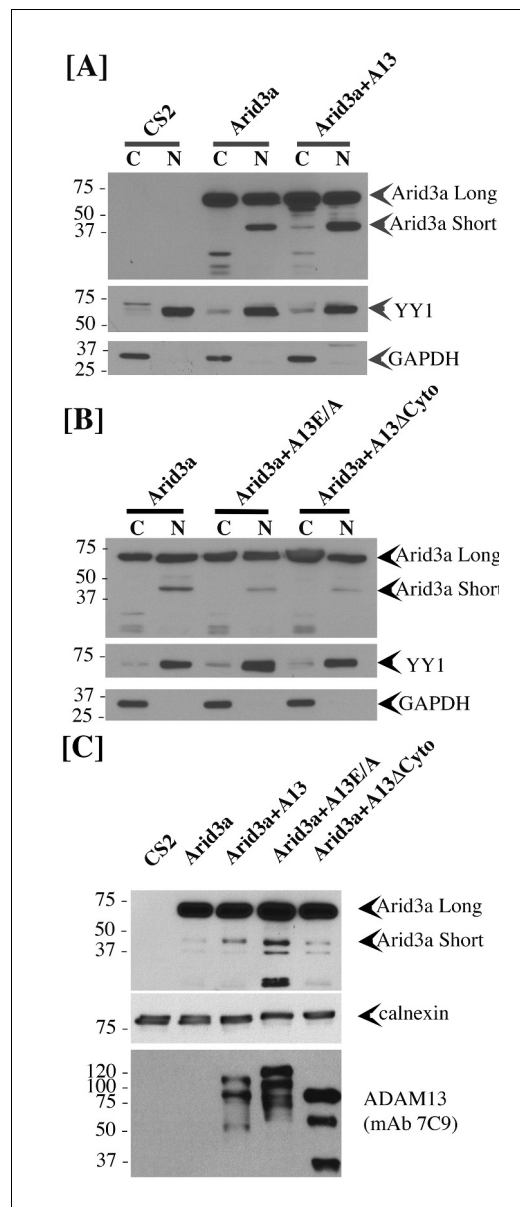


**Figure 10.** adam13 regulates arid3a post-translational modification. Western blot from transfected Hek293T cells. (A–B) cytoplasmic (C) and nuclear (N) extracts from cells transfected with the empty vector (CS2), Arid3a-flag, adam13 (A13) or both. The blots were re-probed with the transcription factor YY1 as a nuclear marker and GAPDH as a cytoplasmic marker. The full-length *Xenopus laevis* Arid3a is detected at approximately 60 kDa (Arid3a Long). A shorter fragment is detected at about 40 kDa (Arid3a Short). (A) Co-transfection of adam13 with Arid3a increases the Arid3a protein level in the cytoplasm by 30% and the shorter fragment of Arid3a in the nucleus by five folds. (B) Co-transfection of Arid3a with the proteolytically inactive mutant adam13 (A13E/A) or the mutant lacking the cytoplasmic domain (A13ΔCyto) does not increase the shorter fragment in the nucleus. (C) Membrane extract from Hek293T cells transfected with Arid3a-flag

Figure 10 continued on next page

suggesting that another control of tfap2α expression is activated later on. This may or may not require the involvement of other ADAM proteases. In particular, it is possible that adam19, which can activate the tfap2α reporter in Hek293T cells may compensate for the loss of adam13 in the CNC. It will be of interest to test if tfap2α expression in mouse is also regulated by ADAM proteases and if this contributes to craniofacial development. Given the conserved ability of the adam19 cytoplasmic domain from mouse and *Xenopus* to functionally replace the adam13 cytoplasmic domain, together with the ability of adam19 to induce the tfap2α reporter, it is tempting to speculate that adam19, which is expressed in mouse CNC and contributes to the cardiac neural crest cell development, could regulate tfap2α to promote CNC migration. While a role for adam13/33 and adam19 in mouse CNC has not been shown, it is possible that the craniofacial phenotypes are subtle and may have been missed in the individual Knock out reports.

Our results show that the extracellular fragment of multiple cadherins and protocadherin can rescue CNC migration. In particular, we have shown that the extracellular fragment of Cadherin-11 can rescue CNC migration in embryos lacking adam13 or expressing a non-cleavable form of cadherin-11 (Abbruzzese et al., 2016). Similarly, the extracellular fragment of pcdh8l partially rescues CNC migration in embryos lacking adam13. It is interesting to note that one can greatly improve the rescue either by injecting full-length pcdh8l together with adam13 lacking a cytoplasmic domain (data not shown). This mutant form of adam13 can cleave pcdh8l but cannot regulate transcription and therefore the level of the protocadherin. Alternatively, greater rescue is also achieved by expressing the EC1-4 fragment of pcdh8l together with tfap2α showing that the transcriptional and proteolytic activity of adam13 can be uncoupled. Why can the various cadherin and protocadherin fragments rescue migration? We have shown that the extracellular fragment of cadherin-11 bind to ErbB2 (EGF receptor 2) and regulates Akt phosphorylation (Mathavan et al., submitted). In cancer cells, the extracellular fragment of E-cadherin can also bind to ErbB2 to promote cell migration (Brouxhon et al., 2014a; Brouxhon et al., 2014b). This suggests that a common structure within the Cadherin/protocadherin extracellular domain can bind and signal through growth factor receptors.

Figure 10 continued

and the adam13 constructs. Co-transfection of Arid3a with adam13 increases the intensity of the 40 kDa Arid3a fragment. This is not observed in the absence of the adam13 cytoplasmic domain. In contrast, a much more significant increase is observed when Arid3a is co-transfected with the A13E/A mutant.

DOI: <https://doi.org/10.7554/eLife.26898.025>

## The larger role of ADAM regulation of transcription

Our results show how ADAMs can regulate transcription via their cytoplasmic domain. Multiple reports have shown ADAM protein in the nuclei (Cousin et al., 2011; Friedrich et al., 2011; Arima et al., 2007). Our previous study has shown that most ADAM cytoplasmic domains can translocate into the nucleus if cleaved from the plasma membrane. For adam13, we have identified a physical interaction with importin  $\beta$ ,

which is known to mediate transport of proteins that do not harbor a canonical nuclear localization signal (Alfandari ms/ms unpublished). Given the essential and conserved role of tfap2 $\alpha$  in craniofacial development (de Croz  et al., 2011; Hoffman et al., 2007; Luo et al., 2003; Martinelli et al., 2011; Meshcheryakova et al., 2015; Van Otterloo et al., 2012; Hong et al., 2014), as well as its ability to reduce the proliferation and migration of multiple cancer cells including those derived from neural crest cells (Su et al., 2014; Li et al., 2010; Bennett et al., 2009; Orso et al., 2007), it will be essential to study the potential regulation of tfap2 $\alpha$  by human ADAM proteins. Our preliminary results show that mouse adam33 and adam12 are also able to induce the tfap2 $\alpha$  reporter when transfected in Hek293T cells even if less efficiently than adam13 or adam19 while Xenopus adam9, 10 and 11 do not (data not shown). A better understanding of the precise regulation of tfap2 $\alpha$  transcription by the various ADAMs will be necessary to determine if they all regulate gene expression by a common mechanism. Similarly, the observed role of adam12 in mediating TGF- $\beta$  signaling, may

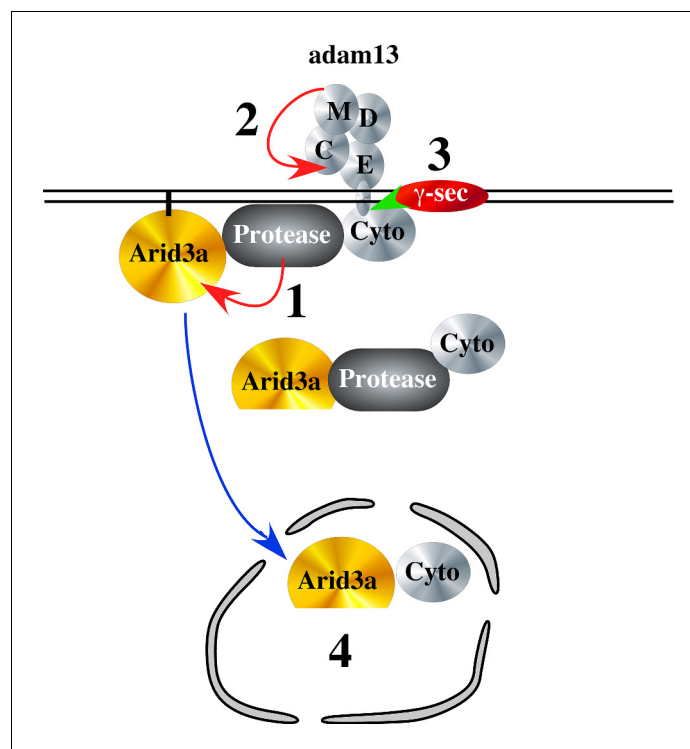


**Figure 11.** Hypothetical model of adam13 function: Adam13 at the membrane may associate with a cytoplasmic protease that cleaves Arid3a (1) to generate the short form seen in Figure 10. Arid3a is localized to lipid raft via its palmytoylation. Once adam13 cleaves itself in the cysteine rich domain (2), gamma secretase cleaves the cytoplasmic domain of adam13 (3), releasing the complex that can translocate in the nucleus to activate tfap2 $\alpha$  transcription.

DOI: <https://doi.org/10.7554/eLife.26898.026>

involve an interaction with arid3a, a protein known to be downstream of the TGF- $\beta$  effector Smad2 (Callery *et al.*, 2005). The fact that both adam12 and arid3a are critical for trophoblast formation (Rhee *et al.*, 2017; Aghababaei *et al.*, 2015; Rhee *et al.*, 2014; Aghababaei *et al.*, 2014) suggests that this functional interaction may be important in multiple cell types to mediate key developmental processes.

## Materials and methods

### Antibodies

The monoclonal antibody to pcdh8l (mAb2F4, RRID:AB\_2687672) was generated against a bacterial fusion protein corresponding to the entire cytoplasmic domain of pcdh8l using standard hybridoma techniques. It recognizes the endogenous protein by western blot and immunofluorescence. 2F4 does not recognize overexpressed protocadherin pcdh8 and pcdh1. The monoclonal antibody to Rpn1 (Mono5, RRID:AB\_2687673) was generated by immunizing BalbC mice with *Xenopus* XTC cells (Pudney *et al.*, 1973). Hybridomas were screened by ELISA on fixed *Xenopus* XTC cells (RRID:CVCL\_5610) and western blot from embryo extracts. Mono5 was further characterized by shot-gun LC/ms/ms of protein immunoprecipitated using Mono5 from embryo extracts. The identity was confirmed by detecting the recombinant *Xenopus* Rpn1 transfected in Hek293T cells (ATCC, CRL-3216 RCB2202). All cell lines were treated with mycoplasma removal agent (MRA, MP-Biomedicals) prior to use. The antibody works by western blot and immunofluorescence on the endogenous *Xenopus* protein. The antibodies to adam13 have been described before. 6615F RRID:AB\_2687671, rabbit polyclonal antibody (Alfandari *et al.*, 1997), DC13, RRID:AB\_2687674 Rabbit polyclonal antibody (Gaultier *et al.*, 2002), gA13, RRID:AB\_2687675 goat polyclonal antibody to the adam13 cytoplasmic domain (Cousin *et al.*, 2011) mAb 4A7, RRID:AB\_2687676 mouse monoclonal antibody to the cytoplasmic domain of adam13 (Abbruzzese *et al.*, 2014). M2, mouse monoclonal antibody to Flag (Sigma, RRID:AB\_439685). Rabbit polyclonal antibody to tfap2 $\alpha$  (LS-C624, LifeSpan BioSciences, RRID:AB\_2199419).

### Morpholinos and DNA constructs

Morpholino antisense oligonucleotides (Gene Tools, Philomath OR) were described elsewhere. MO13 (McCusker *et al.*, 2009), MOtfap2 $\alpha$  (Luo *et al.*, 2003), MO FoxD3 (Sato *et al.*, 2005), MO arid3a (Callery *et al.*, 2005), MOpcdh8l (Rangarajan *et al.*, 2006), 2006), MOSmad2 (Rankin *et al.*, 2011), MO $\beta$ -catenin (Heasman *et al.*, 2000). Full length pcdh8l and tfap2 $\alpha$  in pCS2 were a generous gift from Dr. Thomas Sargent (NIH, Bethesda, MD, USA). The N-terminal flag tag was added in pcdh8l using the In-Fusion kit (Clontech, CA) according to manufacturer's instruction. The EC1-4 construct was produced by inserting a stop codon in the N-terminus tagged pcdh8l after the fourth cadherin repeat. All ADAM constructs are in pCS2 and have been described before. adam9 (McCusker *et al.*, 2009; Cai *et al.*, 1998). adam13, E/A-adam13, A13 $\Delta$ Cyto, GFP-C13 (Cousin *et al.*, 2011; Alfandari *et al.*, 2001), adam19 (Neuner *et al.*, 2009). Monomeric red fluorescent protein (mRFP) in pCS2 was a generous gift from Dr. Jim Smith (Gurdon Institute, Cambridge, United Kingdom). All constructs were sequenced and transfected in Hek293T cells to verify the protein translation, size and surface expression when appropriate.

### Injections

Capped mRNAs were synthesized using SP6 RNA polymerase on DNA linearized with NotI as described before (Cousin *et al.*, 2000). Injectors were calibrated using a 1  $\mu$ l capillary needle (Microcaps, Drumond, PA, USA). The injection pressure was set at 15 psi and the injection time set between 50 and 200 ms to obtain a 5 nl delivery. For the CNC migration assays, the morpholino was injected at the 1 cell stage and mRNAs at 8 cell stage as described previously (Abbruzzese *et al.*, 2014). Embryos were raised at 15°C until tail bud stage (St. 24 to 28) at which time CNC migration was scored for the presence or absence of fluorescent CNC cells in the migration pathways. For each injection the percentage of inhibition was normalized to embryos injected with RFP alone and set to 0% inhibition. All experiments were performed at least three times using different females to determine statistical significance. Each experiment always included a positive control (RFP) and MO13 in addition to all experimental conditions.

## Cell culture and transfection

Hek293T (ATCC, CRL-3216 RCB2202) cells were cultured in RPMI media supplemented with Pen/Strep, L-glutamine, sodium pyruvate, and FBS (10 U/ml, 2 mM; 0.11 mg/ml, 10%; Hyclone, South Logan, UT). Transfections were performed using X-tremeGENE HP DNA Transfection Reagent (Roche, Basel, Switzerland) following the manufacturer's instructions. For pcdh8l shedding assay, cells were incubated with media containing 2% serum for 24 hr after transfection and conditioned media was collected. The shed extracellular domain was purified using Concanavalin-A-agarose (Vector), eluted in reducing Laemmi and blotted using the Flag (M2) monoclonal antibody.

## Animal cap dissection

Embryos were injected at one cell stage with various mRNA constructs or morpholino (quantity provided in figure legends). At stage nine animal caps were dissected and grown in 0.5X Modified Barth's Saline (1XMBS: 88.0 mM NaCl, 1.0 mM KCl, 2.4 mM NaHCO<sub>3</sub>, 15.0 mM HEPES [pH 7.6], 0.3 mM CaNO<sub>3</sub>-4H<sub>2</sub>O, 0.41 mM CaCl<sub>2</sub>-6H<sub>2</sub>O, 0.82 mM MgSO<sub>4</sub>) with gentamicin (50 µg/ml) on agarose plate at 15°C until control embryos reached stage 17 to 20.

## Quantitative PCR

Quantitative real-time PCR was performed as previously described (Neuner *et al.*, 2009). All primers were tested for efficiency. Embryos and explants were collected at the appropriate stage and immediately placed in a guanidinium thiocyanate solution to extract RNA (Roche, RNA isolation Kit). Total RNA was quantified by absorbance at 260 nm using a nanodrop (Thermo Scientific). Polyadenylated RNA was isolated with oligo-dT beads (Qiagen) following manufacturer's instruction. The cDNA was produced using polyA mRNA purified from 10 CNC explants, or 10 animal caps or five embryos using direct cDNA synthesis kit (Quanta) according to manufacturer's instruction. Quantitative PCR was performed using SYBR green (Takara, Kyoto, Japan) to measure mRNA levels of pcdh8l, tfap2α and arid3a. GAPDH was used to normalize total cDNA quantities. Primer sequences are given in **Table 1**. The  $\Delta\Delta\text{CT}$  (Livak and Schmittgen, 2001) technique was used to calculate fold changes. All results are presented as the fold change compare to non-injected.

## Immunoprecipitation and western blots

Hek293T cells, embryos and explants were all extracted in 1XMBS with 1% Triton-X100, protease phosphatase inhibitor cocktail (Thermoscientific) and 5 mM EDTA. Immunoprecipitations were performed using 1–5 µg of antibody bound to proteinA/G-agarose beads (Thermoscientific) either 2 hr at room temperature or overnight at 4°C. Beads were washed three times with the extraction buffer prior to elution with Laemmli buffer. All proteins were separated on 5–22% gradient SDS-PAGE gels and transferred to polyvinylidene fluoride membranes (PVDF, Millipore, Billerica, MA) using a semi-dry transfer apparatus (Hoeffer). pcdh8l glycoprotein was pulled down from total protein extract with concanavalin-A agarose beads (Vector Laboratories, Burlingame, CA). Cytoplasmic and nuclear extracts were performed using the NEper kit (Pierce) following manufacturer's instructions. Purification of total membrane was adapted from (Tamura *et al.*, 2011), Hek293T cells were washed once

**Table 1.**

Target	Sequence 5'–3'
xltfap2α Forward	ATAACAATGCGGTGTCGTCCCTCT
xltfap2α Reverse	AGAGCCTTCTCTGGACTTCTGCAA
xlarid3a Forward	GGAGGCTTGGTGAAGTTATTA
xlarid3a Reverse	ACTGAGTGCGCAGAGTAAAG
xlgapdh Forward	TTAAGACTGCATCAGAGGGCCCAA
xlgapdh Reverse	GGGCAATTCCAGCATCAGCATCAA
xlpcdh8l Forward	TCTCAACTCGTGCTCAAATC
xlpcdh8l Reverse	CCTCTGCTGACCCATTATTC

DOI: <https://doi.org/10.7554/eLife.26898.027>

with PBS and collected by pipetting up and down in ice cold EB (10 mM Hepes pH7.5, 0.3M sucrose, 1 mM EDTA). Cells were collected by spinning at 300 g for 5 min and were then extracted using multiple passages through a 25 g needle (1 ml for a single well of a six well plate) of EB buffer complemented with protease phosphatase inhibitor cocktail (Thermoscientific) and 5 mM EDTA. Intact cells and nuclei were pelleted at 1000 g for 10 min at 4°C. The supernatant were spun at 45,000 rpm/88,000 g (Beckman optima, TLA 100.2) for 30 min at 4°C. The membrane pellet was re-suspended in 100 µl of laemmly buffer. For embryos, 20 embryos were extracted in 500 µl of EB buffer, cell debris and nuclei were spun down at 1,000 g at 4°C for 15 min. The supernatant was then spun at 45,000 rpm/88,000 g at 4C for 30 min to pellet the total membranes.

### Whole mount in situ hybridization

Whole mount in situ hybridization was performed using previously described protocol (*Harland, 1991*). *pcdh8l*, *tfap2α* and *snai2* probes were generated using diogoxigenin-rUTP-label. Images were taken using a Zeiss stereo microscope Lumar-V12 with the Axiovision software package.

### Luciferase activity for *tfap2α* promoter

Hek293T cells were seeded in 6-well plates at 30% confluence the day before transfection. The total amount of DNA per well was adjusted to 1 µg and included 100 ng of the *tfap2α* promoter:luciferase and 100 pg of pRL-CMV. All plasmids were transfected using X-tremeGENE HP as described above. 24 hr after transfection, cells were lysed and processed using the Dual-Luciferase Reporter Assay System protocol (Promega, Madison, WI). For in vivo experiments, 100 pg of the *tfap2α*:luciferase promoter and 10 pg of pRL-CMV were injected at the 8 cell stage in a dorsal animal blastomere. Whole embryos or dissected CNC explants were lysed and processed following the Dual-Luciferase Reporter Assay System protocol. The luminescence signals were measured using a luminometer microplate reader (BMG LABTECH Ortenberg, Germany).

### Statistical methods

For in vivo experiments, each experiment was repeated at least three times on separate days using on average 30 embryos per case per experiment. For Q-PCR and luciferase assays, all experiments were performed at least three times (biological repeats) and each PCR was performed in triplicate. Error bars represent standard error to the mean. One-way ANOVA (non-parametric) was performed using Newman-Keuls to determine statistical significance. Statistically significance was set at \* $p < 0.05$ , \*\* $p < 0.01$  and \*\*\* $p < 0.005$ .

### Acknowledgement

This work was supported by the National Institutes of Health, U.S. Public Health Service, Grant RO1-DE016289 and R24-OD021485 to DA, F31-DE023275 to GA and RO3-DE025692 to HC. The author would like to thank Vanessa Bartollo, Peri Prendergast, Erin Kerdavid, Siddheshwari Advani, Julie Fletcher, Shreyas Srikanth and Brittany Woodland for their contribution to experiments and discussion of this manuscript.

### Additional information

#### Funding

Funder	Grant reference number	Author
National Institute of Dental and Craniofacial Research	F31-DE023275	Genevieve Abbruzzese
National Institute of Dental and Craniofacial Research	RO3-DE025692	Helene Cousin
National Institute of Dental and Craniofacial Research	RO1-DE016289	Dominique Alfandari
National Institutes of Health	R24-OD021485	Dominique Alfandari

The funders had no role in study design, data collection and interpretation, or the decision to submit the work for publication.

#### Author contributions

Vikram Khedgikar, Conceptualization, Formal analysis, Supervision, Investigation, Methodology, Writing—original draft, Writing—review and editing; Genevieve Abbruzzese, Conceptualization, Formal analysis, Methodology, Writing—review and editing; Ketan Mathavan, Formal analysis, Investigation, Methodology, Writing—review and editing; Hannah Szydlo, Validation, Investigation; Helene Cousin, Formal analysis, Supervision, Methodology, Writing—review and editing; Dominique Alfandari, Conceptualization, Formal analysis, Supervision, Funding acquisition, Methodology, Writing—review and editing

#### Author ORCIDs

Dominique Alfandari  <http://orcid.org/0000-0002-0557-1246>

#### Ethics

Animal experimentation: This study was performed in strict accordance with the recommendations in the Guide for the Care and Use of Laboratory Animals of the National Institutes of Health. All of the animals were handled according to approved institutional animal care and use committee (IACUC) protocols (#2015-0029) of the University of Massachusetts Amherst.

#### Decision letter and Author response

Decision letter <https://doi.org/10.7554/eLife.26898.029>

Author response <https://doi.org/10.7554/eLife.26898.030>

## Additional files

#### Supplementary files

- Transparent reporting form

DOI: <https://doi.org/10.7554/eLife.26898.028>

## References

- Abbruzzese G**, Becker SF, Kashef J, Alfandari D. 2016. ADAM13 cleavage of cadherin-11 promotes CNC migration independently of the homophilic binding site. *Developmental Biology* **415**:383–390. DOI: <https://doi.org/10.1016/j.ydbio.2015.07.018>, PMID: 26206614
- Abbruzzese G**, Cousin H, Salicioni AM, Alfandari D. 2014. GSK3 and Polo-like kinase regulate ADAM13 function during cranial neural crest cell migration. *Molecular Biology of the Cell* **25**:4072–4082. DOI: <https://doi.org/10.1091/mbc.E14-05-0970>, PMID: 25298404
- Abbruzzese G**, Gorny AK, Kaufmann LT, Cousin H, Kleino I, Steinbeisser H, Alfandari D. 2015. The Wnt receptor Frizzled-4 modulates ADAM13 metalloprotease activity. *Journal of Cell Science* **128**:1139–1149. DOI: <https://doi.org/10.1242/jcs.163063>, PMID: 25616895
- Aghababaei M**, Hogg K, Perdu S, Robinson WP, Beristain AG. 2015. ADAM12-directed ectodomain shedding of E-cadherin potentiates trophoblast fusion. *Cell Death and Differentiation* **22**:1970–1984. DOI: <https://doi.org/10.1038/cdd.2015.44>, PMID: 25909890
- Aghababaei M**, Perdu S, Irvine K, Beristain AG. 2014. A disintegrin and metalloproteinase 12 (ADAM12) localizes to invasive trophoblast, promotes cell invasion and directs column outgrowth in early placental development. *MHR: Basic Science of Reproductive Medicine* **20**:235–249. DOI: <https://doi.org/10.1093/molehr/gat084>
- Alfandari D**, Cousin H, Gaultier A, Hoffstrom BG, DeSimone DW. 2003. Integrin alpha5beta1 supports the migration of *Xenopus* cranial neural crest on fibronectin. *Developmental Biology* **260**:449–464. DOI: [https://doi.org/10.1016/S0012-1606\(03\)00277-X](https://doi.org/10.1016/S0012-1606(03)00277-X), PMID: 12921745
- Alfandari D**, Cousin H, Gaultier A, Smith K, White JM, Darribère T, DeSimone DW. 2001. *Xenopus* ADAM 13 is a metalloprotease required for cranial neural crest-cell migration. *Current Biology* **11**:918–930. DOI: [https://doi.org/10.1016/S0960-9822\(01\)00263-9](https://doi.org/10.1016/S0960-9822(01)00263-9), PMID: 11448768
- Alfandari D**, Cousin H, Marsden M. 2010. Mechanism of *Xenopus* cranial neural crest cell migration. *Cell Adhesion & Migration* **4**:553–560. DOI: <https://doi.org/10.4161/cam.4.4.12202>, PMID: 20505318

- Alfandari D**, McCusker C, Cousin H. 2009. ADAM function in embryogenesis. *Seminars in Cell & Developmental Biology* **20**:153–163. DOI: <https://doi.org/10.1016/j.semcdb.2008.09.006>, PMID: 18935966
- Alfandari D**, Wolfsberg TG, White JM, DeSimone DW. 1997. ADAM 13: a novel ADAM expressed in somitic mesoderm and neural crest cells during *Xenopus laevis* development. *Developmental Biology* **182**:314–330. DOI: <https://doi.org/10.1006/dbio.1996.8458>, PMID: 9070330
- Arima T**, Enokida H, Kubo H, Kagara I, Matsuda R, Toki K, Nishimura H, Chiyomaru T, Tatarano S, Idesako T, Nishiyama K, Nakagawa M. 2007. Nuclear translocation of ADAM-10 contributes to the pathogenesis and progression of human prostate cancer. *Cancer Science* **98**:1720–1726. DOI: <https://doi.org/10.1111/j.1349-7006.2007.00601.x>, PMID: 17727679
- Bennett KL**, Romigh T, Eng C. 2009. AP-2alpha induces epigenetic silencing of tumor suppressive genes and microsatellite instability in head and neck squamous cell carcinoma. *PLoS One* **4**:e6931. DOI: <https://doi.org/10.1371/journal.pone.0006931>, PMID: 19742317
- Borchers A**, David R, Wedlich D. 2001. *Xenopus* cadherin-11 restrains cranial neural crest migration and influences neural crest specification. *Development* **128**:3049–3060. PMID: 11688555
- Bowes JB**, Snyder KA, Segerdell E, Jarabek CJ, Azam K, Zorn AM, Vize PD. 2010. Xenbase: gene expression and improved integration. *Nucleic Acids Research* **38**:D607–D612. DOI: <https://doi.org/10.1093/nar/gkp953>, PMID: 19884130
- Brouxhon SM**, Kyrkanides S, Teng X, Athar M, Ghazizadeh S, Simon M, O'Banion MK, Ma L. 2014a. Soluble E-cadherin: a critical oncogene modulating receptor tyrosine kinases, MAPK and PI3K/Akt/mTOR signaling. *Oncogene* **33**:225–235. DOI: <https://doi.org/10.1038/onc.2012.563>, PMID: 23318419
- Brouxhon SM**, Kyrkanides S, Teng X, O'Banion MK, Clarke R, Byers S, Ma L. 2014b. Soluble-E-cadherin activates HER and IAP family members in HER2+ and TNBC human breast cancers. *Molecular Carcinogenesis* **53**:893–906. DOI: <https://doi.org/10.1002/mc.22048>, PMID: 23776059
- Cai H**, Krätzschar J, Alfandari D, Hunnicutt G, Blobel CP. 1998. Neural crest-specific and general expression of distinct metalloprotease-disintegrins in early *Xenopus laevis* development. *Developmental Biology* **204**:508–524. DOI: <https://doi.org/10.1006/dbio.1998.9017>, PMID: 9882486
- Callery EM**, Smith JC, Thomsen GH. 2005. The ARID domain protein dril1 is necessary for TGF(beta) signaling in *Xenopus* embryos. *Developmental Biology* **278**:542–559. DOI: <https://doi.org/10.1016/j.ydbio.2004.11.017>, PMID: 15680369
- Cousin H**, Abbruzzese G, Keravid E, Gaultier A, Alfandari D. 2011. Translocation of the cytoplasmic domain of ADAM13 to the nucleus is essential for Calpain8-a expression and cranial neural crest cell migration. *Developmental Cell* **20**:256–263. DOI: <https://doi.org/10.1016/j.devcel.2010.12.009>, PMID: 21316592
- Cousin H**, Abbruzzese G, McCusker C, Alfandari D. 2012. ADAM13 function is required in the 3 dimensional context of the embryo during cranial neural crest cell migration in *Xenopus laevis*. *Developmental Biology* **368**:335–344. DOI: <https://doi.org/10.1016/j.ydbio.2012.05.036>, PMID: 22683825
- Cousin H**, Gaultier A, Bleux C, Darrivière T, Alfandari D. 2000. PACSIN2 is a regulator of the metalloprotease/disintegrin ADAM13. *Developmental Biology* **227**:197–210. DOI: <https://doi.org/10.1006/dbio.2000.9871>, PMID: 11076687
- de Crozé N**, Maczkowiak F, Monsoro-Burq AH. 2011. Reiterative AP2a activity controls sequential steps in the neural crest gene regulatory network. *PNAS* **108**:155–160. DOI: <https://doi.org/10.1073/pnas.1010740107>, PMID: 21169220
- Deardorff MA**, Tan C, Saint-Jeannet JP, Klein PS. 2001. A role for frizzled 3 in neural crest development. *Development* **128**:3655–3663. PMID: 11585792
- Dorsky RI**, Moon RT, Raible DW. 1998. Control of neural crest cell fate by the Wnt signalling pathway. *Nature* **396**:370–373. DOI: <https://doi.org/10.1038/24620>, PMID: 9845073
- Dreymueller D**, Pruessmeyer J, Groth E, Ludwig A. 2012. The role of ADAM-mediated shedding in vascular biology. *European Journal of Cell Biology* **91**:472–485. DOI: <https://doi.org/10.1016/j.ejcb.2011.09.003>, PMID: 22138087
- Friedrich BM**, Murray JL, Li G, Sheng J, Hodge TW, Rubin DH, O'Brien WA, Ferguson MR. 2011. A functional role for ADAM10 in human immunodeficiency virus type-1 replication. *Retrovirology* **8**:32. DOI: <https://doi.org/10.1186/1742-4690-8-32>, PMID: 21569301
- Gaultier A**, Cousin H, Darrivière T, Alfandari D. 2002. ADAM13 disintegrin and cysteine-rich domains bind to the second heparin-binding domain of fibronectin. *Journal of Biological Chemistry* **277**:23336–23344. DOI: <https://doi.org/10.1074/jbc.M201792200>, PMID: 11967265
- Giebeler N**, Zigrino P. 2016. A Disintegrin and Metalloprotease (ADAM): Historical Overview of Their Functions. *Toxins* **8**:122. DOI: <https://doi.org/10.3390/toxins8040122>, PMID: 27120619
- Groves AK**, LaBonne C. 2014. Setting appropriate boundaries: fate, patterning and competence at the neural plate border. *Developmental Biology* **389**:2–12. DOI: <https://doi.org/10.1016/j.ydbio.2013.11.027>, PMID: 24321819
- Harland RM**. 1991. In situ hybridization: an improved whole-mount method for *Xenopus* embryos. *Methods in Cell Biology* **36**:685–695. PMID: 1811161
- Heasman J**, Kofron M, Wylie C. 2000. Beta-catenin signaling activity dissected in the early *Xenopus* embryo: a novel antisense approach. *Developmental Biology* **222**:124–134. DOI: <https://doi.org/10.1006/dbio.2000.9720>, PMID: 10885751
- Hoffman TL**, Javier AL, Campeau SA, Knight RD, Schilling TF. 2007. Tfp2 transcription factors in zebrafish neural crest development and ectodermal evolution. *Journal of Experimental Zoology Part B: Molecular and Developmental Evolution* **308**:679–691. DOI: <https://doi.org/10.1002/jez.b.21189>, PMID: 17724731

- Hong CS**, Devotta A, Lee YH, Park BY, Saint-Jeannet JP. 2014. Transcription factor AP2 epsilon (Tfap2e) regulates neural crest specification in *Xenopus*. *Developmental Neurobiology* **74**:894–906. DOI: <https://doi.org/10.1002/dneu.22173>, PMID: 24616412
- Karpinka JB**, Fortriede JD, Burns KA, James-Zorn C, Ponferrada VG, Lee J, Karimi K, Zorn AM, Vize PD. 2015. Xenbase, the *Xenopus* model organism database; new virtualized system, data types and genomes. *Nucleic Acids Research* **43**:D756–D763. DOI: <https://doi.org/10.1093/nar/gku956>, PMID: 25313157
- Kashef J**, Köhler A, Kuriyama S, Alfandari D, Mayor R, Wedlich D. 2009. Cadherin-11 regulates protrusive activity in *Xenopus* cranial neural crest cells upstream of Trio and the small GTPases. *Genes & Development* **23**:1393–1398. DOI: <https://doi.org/10.1101/gad.519409>, PMID: 19528317
- Langhe RP**, Gudzenko T, Bachmann M, Becker SF, Gonnermann C, Winter C, Abbruzzese G, Alfandari D, Kratzer MC, Franz CM, Kashef J. 2016. Cadherin-11 localizes to focal adhesions and promotes cell-substrate adhesion. *Nature Communications* **7**:10909. DOI: <https://doi.org/10.1038/ncomms10909>, PMID: 26952325
- Li X**, Glubrecht DD, Godbout R. 2010. AP2 transcription factor induces apoptosis in retinoblastoma cells. *Genes, Chromosomes and Cancer* **49**:n/a–30. DOI: <https://doi.org/10.1002/gcc.20790>, PMID: 20607706
- Livak KJ**, Schmittgen TD. 2001. Analysis of relative gene expression data using real-time quantitative PCR and the 2<sup>-</sup>(Delta Delta C(T)) Method. *Methods* **25**:402–408. DOI: <https://doi.org/10.1006/meth.2001.1262>, PMID: 11846609
- Lu X**, Lu D, Scully M, Kakkar V. 2008. ADAM proteins - therapeutic potential in cancer. *Current Cancer Drug Targets* **8**:720–732. PMID: 19075595
- Luo T**, Lee YH, Saint-Jeannet JP, Sargent TD. 2003. Induction of neural crest in *Xenopus* by transcription factor AP2alpha. *PNAS* **100**:532–537. DOI: <https://doi.org/10.1073/pnas.0237226100>, PMID: 12511599
- Luo T**, Matsuo-Takasaki M, Thomas ML, Weeks DL, Sargent TD. 2002. Transcription factor AP-2 is an essential and direct regulator of epidermal development in *Xenopus*. *Developmental Biology* **245**:136–144. DOI: <https://doi.org/10.1006/dbio.2002.0621>, PMID: 11969261
- Luo T**, Zhang Y, Khadka D, Rangarajan J, Cho KW, Sargent TD. 2005. Regulatory targets for transcription factor AP2 in *Xenopus* embryos. *Development, Growth and Differentiation* **47**:403–413. DOI: <https://doi.org/10.1111/j.1440-169X.2005.00809.x>, PMID: 16109038
- Martinelli M**, Masiero E, Carinci F, Morselli PG, Palmieri A, Girardi A, Baciliero U, Scapoli L. 2011. Evidence of an involvement of TFAP2A gene in non-syndromic cleft lip with or without cleft palate: an Italian study. *International Journal of Immunopathology and Pharmacology* **24**:7–10. DOI: <https://doi.org/10.1177/039463201102405202>, PMID: 21781438
- McCusker C**, Cousin H, Neuner R, Alfandari D. 2009. Extracellular cleavage of cadherin-11 by ADAM metalloproteases is essential for *Xenopus* cranial neural crest cell migration. *Molecular Biology of the Cell* **20**:78–89. DOI: <https://doi.org/10.1091/mbc.E08-05-0535>, PMID: 18946084
- Meshcheryakova TI**, Zinchenko RA, Vasilyeva TA, Marakhonov AV, Zhyliina SS, Petrova NV, Kozhanova TV, Belenikin MS, Petrin AN, Mutovin GR. 2015. A clinical and molecular analysis of branchio-oculo-facial syndrome patients in Russia revealed new mutations in TFAP2A. *Annals of Human Genetics* **79**:148–152. DOI: <https://doi.org/10.1111/ahg.12098>, PMID: 25590586
- Milet C**, Monsoro-Burq AH. 2012. Neural crest induction at the neural plate border in vertebrates. *Developmental Biology* **366**:22–33. DOI: <https://doi.org/10.1016/j.ydbio.2012.01.013>, PMID: 22305800
- Monsoro-Burq AH**, Fletcher RB, Harland RM. 2003. Neural crest induction by paraxial mesoderm in *Xenopus* embryos requires FGF signals. *Development* **130**:3111–3124. DOI: <https://doi.org/10.1242/dev.00531>, PMID: 12783784
- Moody SA**. 1987. Fates of the blastomeres of the 16-cell stage *Xenopus* embryo. *Developmental Biology* **119**:560–578. DOI: [https://doi.org/10.1016/0012-1606\(87\)90059-5](https://doi.org/10.1016/0012-1606(87)90059-5), PMID: 3803718
- Neuner R**, Cousin H, McCusker C, Coyne M, Alfandari D. 2009. *Xenopus* ADAM19 is involved in neural, neural crest and muscle development. *Mechanisms of Development* **126**:240–255. DOI: <https://doi.org/10.1016/j.mod.2008.10.010>, PMID: 19027850
- Orso F**, Fassetta M, Penna E, Solero A, De Filippo K, Sismondi P, De Bortoli M, Taverna D. 2007. The AP-2alpha transcription factor regulates tumor cell migration and apoptosis. *Advances in Experimental Medicine and Biology* **604**:87–95. DOI: [https://doi.org/10.1007/978-0-387-69116-9\\_6](https://doi.org/10.1007/978-0-387-69116-9_6), PMID: 17695722
- Owens ND**, Blitz IL, Lane MA, Patrushev I, Overton JD, Gilchrist MJ, Cho KW, Khokha MK. 2016. Measuring Absolute RNA Copy Numbers at High Temporal Resolution Reveals Transcriptome Kinetics in Development. *Cell Reports* **14**:632–647. DOI: <https://doi.org/10.1016/j.celrep.2015.12.050>, PMID: 26774488
- Pollheimer J**, Fock V, Knöfler M. 2014. Review: the ADAM metalloproteinases - novel regulators of trophoblast invasion? *Placenta* **35 Suppl**:S57–S63. DOI: <https://doi.org/10.1016/j.placenta.2013.10.012>, PMID: 24231445
- Prieur A**, Nacerddine K, van Lohuizen M, Peeper DS. 2009. SUMOylation of DRIL1 directs its transcriptional activity towards leukocyte lineage-specific genes. *PLoS One* **4**:e5542. DOI: <https://doi.org/10.1371/journal.pone.0005542>, PMID: 19436740
- Pudney M**, Varma MG, Leake CJ. 1973. Establishment of a cell line (XTC-2) from the South African clawed toad, *Xenopus laevis*. *Experientia* **29**:466–467. DOI: <https://doi.org/10.1007/BF01926785>, PMID: 4708349
- Rangarajan J**, Luo T, Sargent TD. 2006. PCNS: a novel protocadherin required for cranial neural crest migration and somite morphogenesis in *Xenopus*. *Developmental Biology* **295**:206–218. DOI: <https://doi.org/10.1016/j.ydbio.2006.03.025>, PMID: 16674935
- Rankin SA**, Kormish J, Kofron M, Jegga A, Zorn AM. 2011. A gene regulatory network controlling hhex transcription in the anterior endoderm of the organizer. *Developmental Biology* **351**:297–310. DOI: <https://doi.org/10.1016/j.ydbio.2010.11.037>, PMID: 21215263

- Reiss K, Saftig P.** 2009. The "a disintegrin and metalloprotease" (ADAM) family of sheddases: physiological and cellular functions. *Seminars in Cell & Developmental Biology* **20**:126–137. DOI: <https://doi.org/10.1016/j.semcdb.2008.11.002>, PMID: 19049889
- Rhee C, Edwards M, Dang C, Harris J, Brown M, Kim J, Tucker HO.** 2017. ARID3A is required for mammalian placenta development. *Developmental Biology* **422**:83–91. DOI: <https://doi.org/10.1016/j.ydbio.2016.12.003>, PMID: 27965054
- Rhee C, Lee BK, Beck S, Anjum A, Cook KR, Popowski M, Tucker HO, Kim J.** 2014. Arid3a is essential to execution of the first cell fate decision via direct embryonic and extraembryonic transcriptional regulation. *Genes & Development* **28**:2219–2232. DOI: <https://doi.org/10.1101/gad.247163.114>, PMID: 25319825
- Ruff M, Leyme A, Le Cann F, Bonnier D, Le Seyec J, Chesnel F, Fattet L, Rimokh R, Baffet G, Théret N.** 2015. The Disintegrin and Metalloprotease ADAM12 Is Associated with TGF- $\beta$ -Induced Epithelial to Mesenchymal Transition. *PLoS One* **10**:e0139179. DOI: <https://doi.org/10.1371/journal.pone.0139179>, PMID: 26407179
- Sandelin A, Alkema W, Engström P, Wasserman WW, Lenhard B.** 2004. JASPAR: an open-access database for eukaryotic transcription factor binding profiles. *Nucleic Acids Research* **32**:91D–94. DOI: <https://doi.org/10.1093/nar/gkh012>, PMID: 14681366
- Sato T, Sasai N, Sasai Y.** 2005. Neural crest determination by co-activation of Pax3 and Zic1 genes in *Xenopus* ectoderm. *Development* **132**:2355–2363. DOI: <https://doi.org/10.1242/dev.01823>, PMID: 15843410
- Schiffmacher AT, Padmanabhan R, Jhingory S, Taneyhill LA.** 2014. Cadherin-6B is proteolytically processed during epithelial-to-mesenchymal transitions of the cranial neural crest. *Molecular Biology of the Cell* **25**:41–54. DOI: <https://doi.org/10.1091/mbc.E13-08-0459>, PMID: 24196837
- Schmidt C, Kim D, Ippolito GC, Naqvi HR, Probst L, Mathur S, Rosas-Acosta G, Wilson VG, Oldham AL, Poenie M, Webb CF, Tucker PW.** 2009. Signalling of the BCR is regulated by a lipid rafts-localised transcription factor, Bright. *The EMBO Journal* **28**:711–724. DOI: <https://doi.org/10.1038/emboj.2009.20>, PMID: 19214191
- Schneider M, Huang C, Becker SF, Gradl D, Wedlich D.** 2014. Protocadherin PAPC is expressed in the CNC and can compensate for the loss of PCNS. *Genesis* **52**:120–126. DOI: <https://doi.org/10.1002/dvg.22736>, PMID: 24339193
- Su W, Xia J, Chen X, Xu M, Nie L, Chen N, Gong J, Li X, Zhou Q.** 2014. Ectopic expression of AP-2 $\alpha$  transcription factor suppresses glioma progression. *International Journal of Clinical and Experimental Pathology* **7**:8666–8674. PMID: 25674231
- Suzuki M, Okuyama S, Okamoto S, Shirasuna K, Nakajima T, Hachiya T, Nojima H, Sekiya S, Oda K.** 1998. A novel E2F binding protein with Myc-type HLH motif stimulates E2F-dependent transcription by forming a heterodimer. *Oncogene* **17**:853–865. DOI: <https://doi.org/10.1038/sj.onc.1202163>, PMID: 9780002
- Tamura T, Cormier JH, Hebert DN.** 2011. Characterization of early EDEM1 protein maturation events and their functional implications. *Journal of Biological Chemistry* **286**:24906–24915. DOI: <https://doi.org/10.1074/jbc.M111.243998>, PMID: 21632540
- Tribulo C, Aybar MJ, Nguyen VH, Mullins MC, Mayor R.** 2003. Regulation of Msx genes by a Bmp gradient is essential for neural crest specification. *Development* **130**:6441–6452. DOI: <https://doi.org/10.1242/dev.00878>, PMID: 14627721
- Van Otterloo E, Li W, Bonde G, Day KM, Hsu MY, Cornell RA.** 2010. Differentiation of zebrafish melanophores depends on transcription factors AP2 alpha and AP2 epsilon. *PLoS Genetics* **6**:e1001122. DOI: <https://doi.org/10.1371/journal.pgen.1001122>, PMID: 20862309
- Van Otterloo E, Li W, Garnett A, Cattell M, Medeiros DM, Cornell RA.** 2012. Novel Tfap2-mediated control of soxE expression facilitated the evolutionary emergence of the neural crest. *Development* **139**:720–730. DOI: <https://doi.org/10.1242/dev.071308>, PMID: 22241841
- Wei S, Xu G, Bridges LC, Williams P, White JM, DeSimone DW.** 2010. ADAM13 induces cranial neural crest by cleaving class B Ephrins and regulating Wnt signaling. *Developmental Cell* **19**:345–352. DOI: <https://doi.org/10.1016/j.devcel.2010.07.012>, PMID: 20708595